



Storm Gloria (2020): joint probability of multiple flood hazards and compound events in a paradigmatic Mediterranean event

Montserrat Llasat-Botija^{1,2}, Raül Marcos-Matamoros¹, Maria Aguilera-Vidal³, José Antonio Jimenez³,
María Carmen Llasat^{1,2}

5 ¹GAMA, Department of Applied Physics, Universitat de Barcelona, Barcelona, 08028, Spain

²IdRA, Water Research Institute, Universitat de Barcelona, Barcelona, 08028, Spain

³Laboratori d'Enginyeria Marítima, Universitat Politècnica de Catalunya, BarcelonaTech, Barcelona, 08034, Spain

Correspondence to: Montserrat Llasat-Botija (mllasat@meteo.ub.edu)

Abstract. Compound flooding arises when multiple hydrometeorological drivers co-occur and interact, amplifying
10 risk beyond that expected from individual hazards. This work analyses Storm Gloria (19–25 January 2020, E Spain)
as a paradigmatic compound event in the Mediterranean region. The coastal strip considered here extends for 1,609
km (from the French border to Málaga) and includes 8.4 million inhabitants in 12,167 km². The event affected 770
municipalities, caused 13 fatalities and four missing persons and generated about EUR₂₀₂₂ 204 million in Spain's
Insurance Compensation (CCS) payouts. The analysis combines daily precipitation ($P_{(24h)}$; 662 AEMET rain
15 gauges), maximum wind gusts (140 stations), and significant wave height (H_s ; 50 SIMAR/CoExMed points) with
municipality-level CCS compensation data. The event window is objectively defined (≥ 40 mm day⁻¹ at ≥ 2
stations), and hazard severity is mapped using operational thresholds ($P_{24h} = 40/100/200$ mm; $H_s = 2/5/7$ m; wind
gusts $\approx 70/90/100$ km h⁻¹). Multivariate (river and sea flooding at the Tordera River mouth) and spatially
compounding (flooding in the Júcar basin and sea storm in the Gulf of Jávea) cases are quantified through a two-
20 sided conditional framework and copulas in two areas located in the northern and central part of the study region,
respectively, whereas the temporally compounding case is evaluated empirically from heavy-rainfall episodes in
the Segura basin, located in the southern part. Results indicate that, for the first case, the return period of the
maximum recorded precipitation is estimated at 24 years; however, when the compound event—where wave action
hindered the discharge of the Tordera River into the sea—is taken into account, the estimated return period
25 increases to 85 years. In the second case, it goes from 1.5 years to 72 years, while in the third, the return period
corresponding to the time sequence of three heavy rainfall events in the same basin, becomes 22 years. Overall, the
largest compensation values tend to occur where hazard levels are highest, although exposure, vulnerability, and
insurance coverage modulate the final impacts. This integrated workflow (objective event definition,
threshold-based hazard mapping, copula-based joint recurrence, and impact linkage) provides a transferable,



30 practice-ready template for compound-aware coastal risk assessment in Mediterranean settings and other coastal
regions.

1 Introduction

Between 19 and 25 January 2020, Storm Gloria severely affected eastern Spain. This storm developed south of the
35 Iberian Peninsula (IP) and was the seventh named storm of the 2019–2020 season (AEMET, 2025). Owing to its
spatial extent and its intensity, the unusual time of year it occurred, and the multiple hazards recorded, Gloria is
widely regarded as an exceptional event. It affected wide areas of Catalonia, the Valencian Community, the Region
of Murcia, parts of Andalusia, Aragon, and the Balearic Islands. The episode was characterised by persistent heavy
rainfall, river flooding, flash floods, strong winds, severe maritime conditions, coastal erosion, thunderstorms, hail,
40 snowfalls, and numerous landslides. According to the Insurance Compensation Consortium (“Consortio de
Compensación de Seguros”, CCS), total economic losses across Spain exceeded EUR₂₀₂₂ 204 million (EUR₂₀₂₂
expresses the economic amount adjusted to the value it would have in 2022). In total, approximately 770
municipalities were affected, and the event caused 13 confirmed fatalities and four missing persons (AEMET,
2025; Luján López, 2022).

45

The Gloria event is widely considered as a paradigmatic compound event. The analysis of such types of events
from a “compound” perspective is not new. The report “Managing the Risks of Extreme Events and Disasters to
Advance Climate Change Adaptation” (IPCC, 2012) was one of the first to consolidate the concept of “compound
events”, defining them as: “(1) two or more extreme events occurring simultaneously or successively, (2)
50 combinations of extreme events with underlying conditions that amplify the impact of the events, or (3)
combinations of events that are not themselves extremes but lead to an extreme event or impact when combined.
Contributing events can be similar (clustered multiple events) or of different types”. Shortly thereafter, Leonard et
al. (2014) proposed a framework for the systematic analysis of such events using influence diagrams for defining,
mapping, analysing, modelling, and communicating the risk of the compound event. Since then, interest in this
55 topic has grown significantly within the scientific community due to the substantial socio-economic impacts of
compound events and their potential increase under climate change (Moftakhari et al., 2017; Bevacqua et al., 2019).
Well-documented examples include floods driven by the occurrence of intense coastal rainfall and maritime storms,
known as compound coastal flood events (Sanuy et al., 2021; Romero-Martín et al., 2025), compound drought-
heatwave events (Shan et al., 2024), and co-occurrence of extreme weather conditions in geographically distinct
60 regions (Leeding et al., 2022). In the European context, the Mediterranean coast is considered a hotspot for



compound events both because of their high frequency and because of the high population density and assets along the coastline (MedECC, 2024). To better characterise them, Zscheischler et al. (2020) proposed a classification of compound events into four types:

- 65 - Preconditioned events: a pre-existing, climate-driven condition, leading to the occurrence or amplification of an impact due to one or more hazards.
- Multivariate events: events where different climate drivers and/or hazards occur simultaneously causing impacts in the same geographical area.
- Temporally compounding events: events that occur consecutively over time and affect the same geographical region in a way that causes greater damage than if they had occurred in isolation.
- 70 - Spatially compounding events: events where the same or different hazards occur in multiple connected locations within a limited time window.

A fifth category can be added to the four types of compound events: cascading events. A cascading hazard refers to a primary event that triggers a chain of consequences, which may range from moderate to severe (NASEM, 75 2022). In such cases, the “hazards” are causally linked as one or more occur because of previous hazards. For example, the interruption of railway traffic due to the collapse of a bridge over a river, or an industrial chemical spill resulting from river flooding, would both be considered cascading events. Thus, the recent fall of a wall on a train that produced one fatality on 20 January 2026, was a direct consequence of the large accumulation of water in the subsoil after an anomalous period of continuous heavy rains in Catalonia (NE Spain).

80

The study of Storm Gloria across the entire affected region is a particularly suitable case because, despite having already been analysed from several disciplinary perspectives, most studies have focused on Catalonia or on a single hazard of the event. Existing work has addressed the hydrometeorological characteristics of the storm (SMC, 2020; OCCO, 2020; Palau et al., 2022; Bolaños-Sánchez et al., 2023), broader socio-economic and emergency- 85 management aspects (Llasat et al., 2023), and specific geological, coastal, or social effects (González, 2020; Santasusagna Riu and Tort Donada, 2020; Canals and Miranda, 2020; Pintó et al., 2020). Other studies have examined the marine component and forecasting performance in greater detail (Amores et al., 2020; De Alfonso et al., 2021; Sotillo et al., 2021; Pérez-Gómez et al., 2021). However, no previous study has jointly analysed the full coastal sector affected by Gloria, over more than 1,600 km of coastline, from an explicit compound-event 90 perspective.



In this context, the present study analyses the evolution and impacts of Storm Gloria as a compound flood event affecting the western Mediterranean coast of the IP. Within the overall episode, several sub-events can be interpreted using the compound-event typology proposed by Zscheischler et al. (2020), together with cascading sequences. Three representative sub-events were selected for detailed analysis. To this end, the paper begins with a description of the study area and the data sources used. The Methodology section then outlines the thresholds and criteria used to characterise key meteorological and oceanographic variables, and describes the probabilistic framework applied to quantify both the co-occurrence and the temporal sequencing of the contributing phenomena. This is followed by the results section which presents (i) the specific realisations of the three selected compound-sub-event types identified during Storm Gloria and (ii) an assessment of the main societal and environmental impacts, providing an integrated measure of the event's overall severity. Finally, the Conclusions synthesise the principal findings and their implications for compound-event risk assessment.

2 Study area and data sources

2.1 Study area

The geographical scope of this study comprises the following provinces of the Spanish Mediterranean coast of the IP (Fig. 1): Girona, Barcelona and Tarragona in Catalonia (CAT); Castellón, Valencia and Alicante in the Valencian Community (CVAL); the Region of Murcia (MU) and Almería, Granada and Málaga in Andalusia (AND). Together, these ten provinces account for 83,239 km², about 16% of the Spanish peninsular land area, and concentrate 39% of its population (17.2 million inhabitants). The coastal strip itself includes 174 municipalities distributed along 1,609 km of coastline and covers 12,167 km² (approximately 15% of the total area of the ten provinces), hosting 48% of their population. This underlines the high population concentration in coastal areas (Table 1).



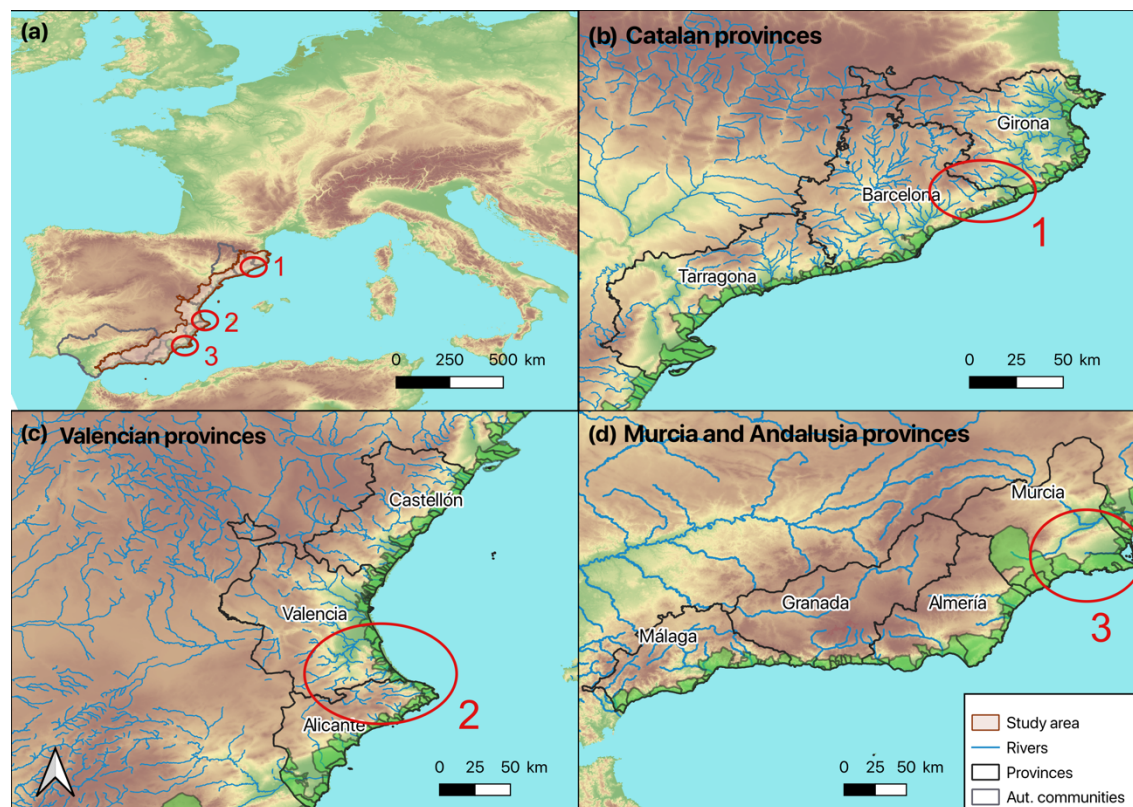
Table 1: Characteristics of the study region, both for the provinces as a whole and only for the coastal part: area (km²), population (2022), number of municipalities (N mun.) and number of littoral municipalities (N lit.mun.). The GDP per capita at the provincial level in EUR₂₀₂₂ is also indicated as well as at the Spanish level.

125

<i>Autonomous Community</i>	<i>Provinces</i>	Provinces				Coastal municipalities		
		<i>Area (km²)</i>	<i>Population (2022)</i>	<i>GDP/capita (EUR₂₀₂₂)</i>	<i>N mun.</i>	<i>N lit. mun.</i>	<i>Area (km²)</i>	<i>Population (2022)</i>
Catalonia	Girona	5,910	793,478	32,829	221	22	662	253,166
	Barcelona	7,728	5,727,615	33,369	311	27	474	2,637,967
	Tarragona	6,303	830,075	32,150	184	21	1,009	434,519
Valencian Community	Castellón	6,632	590,616	29,198	135	16	919	375,642
	Valencia	10,806	2,605,757	26,009	266	24	707	1,164,545
	Alicante	5,817	1,901,594	21,622	141	19	1,658	1,124,539
Murcia Region	Murcia	11,313	1,531,878	24,334	45	8	2,946	483,769
Andalusia	Almería	8,775	740,534	21,999	103	13	1,959	519,445
	Granada	12,647	921,987	20,349	174	10	448	116,824
	Málaga	7,308	1,717,504	21,444	103	14	1,385	1,326,398
TOTAL		83,239	17,361,038	28,748 (Spain)	1,683	174	12,167	8,436,814

The Spanish Mediterranean region of the Iberian Peninsula is characterised by the presence of mountain ranges running roughly parallel to the coastline. These include the *Cordilleras* Litoral and Prelitoral in Catalonia, the *Sistema Ibérico* in the Valencian Community, and the *Sistema Bético* in Murcia and Mediterranean Andalusia (Fig. 1). In some areas, such as the Valencian Community, these mountain systems extend almost directly to the coast, resulting in narrow coastal plains. The region’s hydrographic network is dominated by a high density of ephemeral and torrential watercourses (locally known as “*rieres*” or “*ramblas*”), which respond rapidly to intense rainfall.

130



135 **Figure 1: Localisation and main geographical features of the study area (a) and the provinces in the autonomous communities (b, c and d). Coastal municipalities are shaded in green. Locations of the three compound sub-events are shown: multivariate in the Tordera River mouth (1); spatially compounding on the coast of Valencia (2); and temporally compound in los Alcázares (3).**

The most important economic sectors are tourism and construction, both of which contribute to strong urban pressure along the coast (CGRD, 2019). Other relevant sectors are agriculture (for example, intensive greenhouse cultivation in Almería), industry and logistics (particularly around Valencia and Tarragona), and major business and innovation hubs (notably in Barcelona). A clear territorial gradient in GDP per capita is observed along the Mediterranean coast of the IP: values exceed the national average in the northern provinces (Barcelona, Girona, Tarragona, and Castellón), but tend to decrease towards the south. This decline begins in Valencia, where GDP per capita already falls below the national average.

145

2.2 Data sources

To analyse and quantify the precipitation and wind conditions during the period from 19 to 25 January 2020, observational data were obtained from automatic weather stations operated by the Spanish Meteorological Agency (AEMET, *Agencia Estatal de Meteorología*) within the study area. For precipitation, daily accumulated rainfall



150 (P24h) was collected from 662 stations. For wind, maximum daily wind gusts were analysed using data from 140
automatic stations. Wave conditions were assessed using offshore data from 50 measurement points in the SIMAR
database, maintained by Puertos del Estado (<http://www.puertos.es/es-es/oceanografia>). In addition, wave hindcast
data from the “Coastal Extremes in the Mediterranean Sea” (CoExMed) model nodes (Toomey et al., 2022) were
used to further characterise marine conditions during the event.

155

To identify the impacts and phenomena associated with the episode, a wide range of official sources were consulted,
including reports, press releases, approved decrees, and technical studies, as well as newspaper archives (e.g. La
Vanguardia, MyNews, EFE Prensa, and regional and local press). Social media platforms and specialised weather
websites managed by meteorology enthusiasts were used only as complementary sources.

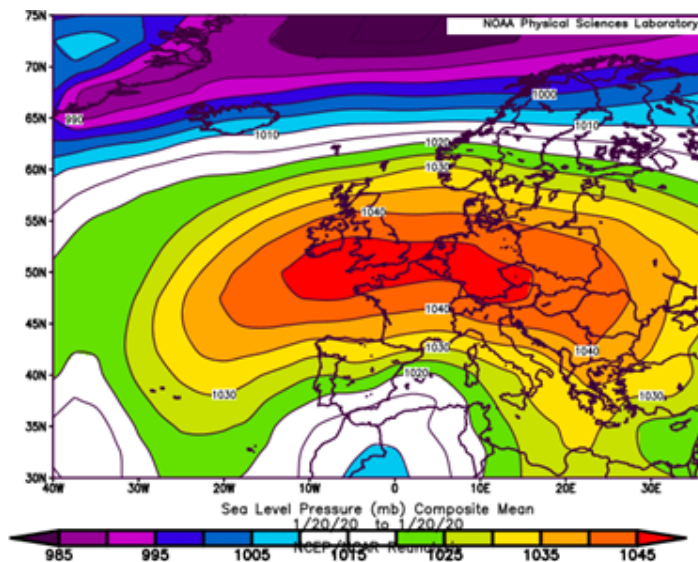
160

To assess the economic impact, data provided by the Insurance Compensation Consortium (CCS) were used. These
data include compensation payments associated with extraordinary flooding, sea storms, and Atypical Cyclonic
Storms (TCA), the latter defined as events involving wind gusts above 120 km h^{-1} .

165 **3 Methodology**

3.1. Event definition and threshold selection

170 Between 19 and 25 January 2020, a low-pressure system south of the IP (Gloria) remained blocked by a strong
anticyclone extending from the British Isles towards France (Fig. 2). This synoptic configuration produced
persistent easterly flow over the eastern Iberian Peninsula, a strong pressure gradient, and sustained onshore
advection of warm, moisture-laden Mediterranean air. A loft, a cold upper-level disturbance enhanced instability
and ascent. Where this flow encountered coastal mountain ranges, especially from Valencia to Catalonia, it
triggered intense orographic precipitation. In other sectors, the cold air also favoured snowfall. The same pressure
gradient generated severe winds and high waves along large parts of the coast. Together, these ingredients explain
both the exceptional intensity and the unusually broad spatial footprint of the event.



175

Figure 2: Reanalysis of sea level pressure on January 20, 2020. Source: NCEP/NCAR Reanalysis, Boulder, Colorado, USA, www.esrl.noaa.gov/psd/

The initial and final dates of the event were first identified from previous reports and analyses (SMC, 2020; González, 2020; AEMET, 2020a). However, discrepancies were noted among the different sources regarding the exact temporal limits of the episode. To ensure consistency, the event window used in this paper was defined objectively as the period during which daily precipitation exceeded 40 mm in at least two stations within the study area. Under this criterion, Storm Gloria lasted from 19 to 25 January 2020. This definition was further supported by a review of synoptic reanalysis maps, which confirmed that the rainfall observed on 25 January can be attributed to the same meteorological system and, thus, included within the event.

To characterise the event from a meteorological perspective, the observations recorded between 19 and 25 January 2020 were classified into three severity categories based on previous studies and on operational thresholds used by AEMET and SMC (*Servei Meteorològic de Catalunya* or Meteorological Service of Catalonia) (Table 2). This framework allows moderate, significant, and extreme values to be distinguished consistently across the study area.

For 24 h precipitation (P24h), thresholds of 40, 100, and 200 mm were adopted. The minimum threshold of 40 mm has been widely used in studies of intense rainfall and flooding in the Mediterranean region (Cortès et al., 2019; Sanuy et al., 2021), while the 100 and 200 mm thresholds are also commonly used as operational reference levels



195 for heavy-rainfall warnings in the study region. For maximum wind gusts, thresholds of about 70, 90, and 100 km
h⁻¹ were selected from AEMET warning criteria and previous studies (Amaro et al., 2010; Romero-Martín et al.,
2025). Wave severity was characterised using the daily maximum significant wave height (H_s), computed from
hourly values between 00:00 and 24:00 UTC. H_s is defined as the average height of the highest one-third of the
waves. For spatial attribution, each SIMAR station was associated with its nearest coastal municipalities, allowing
200 daily wave-height values to be assigned to the 174 coastal municipalities in the study area. For consistency across
the whole study area, thresholds of 2, 5, and 7 m were adopted. The first threshold is consistent with storm
conditions along the Catalan coast and is conservative for sectors where lower operational thresholds are sometimes
used, such as 1–1.5 m in the Andalusia–Valencia sector (ROM, 1991). The higher thresholds are consistent with
values commonly used in the literature to distinguish severe and extreme wave conditions (Del Río et al., 2012;
205 Mendoza et al., 2011; Romero-Martín et al., 2025), thereby providing three robust and spatially consistent
categories of wave severity.

Table 2: Thresholds for each category

Category	Precipitation (mm, 24h)	Max. wind gust (km h ⁻¹)	Wave height (m)
1	40	70	2
2	100	90	5
3	200	100	7

210 3.2 Impact assessment

To assess the damage caused by the event, the total compensation paid by the CCS for insured property was
calculated for each municipality within the study area. CCS data provide a useful proxy for economic impact and
have already been used in previous studies (e.g. Cortès et al., 2018; Rivas et al., 2022). Since CCS provides records
at the postal code level, the data were aggregated to municipality level following the approach of Cortès et al.
215 (2018): (1) selecting claims dated between the first day of the event and 7 days after its end, and (2) summing the
selected claims within each municipality. All monetary values were converted to constant EUR₂₀₂₂ using the
Consumer Price Index, unless otherwise stated.

3.3 Probabilistic analysis of selected compound sub-events



220 Storm Gloria was a long-lasting, spatially extensive episode involving interacting hazards such as heavy rainfall,
high waves, strong winds, snowfall, hail, and local landslides. Although the episode as a whole can be described
as a compound event, its internal structure can also be decomposed into sub-events representative of different
compound-event typologies. Three sub-events were selected for detailed analysis based on their representativeness,
data availability, and impact relevance: a multivariate case at the Tordera mouth, a spatially compounding inland–
225 coastal case linking the Júcar basin and the Gulf of Jávea, and a temporally compounding case associated with
repeated impacts in Los Alcázares.

For the multivariate and spatially compounding cases, the probability of the selected configurations was assessed
using the two-sided conditional framework of Wahl et al. (2015) to estimate joint return periods. Two event types
230 were defined: (i) wave-dominated events, denoted (Hs_99.5, P24h), in which an extreme Hs event was paired with
the highest co-occurring P24h within the selected subregion; and (ii) rain-dominated events, denoted (P24h_98,
Hs), in which an extreme P24h event was paired with the highest co-occurring Hs. Extremes of the conditioning
variable were individually modelled with a peaks-over-threshold Generalized Pareto distribution. For the paired
variable, several candidate distributions (exponential, two-parameter gamma, lognormal, Weibull, and Tweedie)
235 were fitted and the best one was selected using the Akaike Information Criterion (AIC). Dependence between
variables was modelled with copulas (Coles and Tawn, 1991; Coles et al., 1999; Genest and Favre, 2007), using
the VineCopula R package (Nagler, 2012).

By combining the two conditional bivariate models (one rainfall-conditioned and one wave-conditioned) we
240 estimated the joint return period of the multivariate and spatially compounding cases. This was done using the
observed values during the Gloria storm and the time series at each location corresponding to the three cases
analysed: multivariate, spatially and temporally compound.

4 Results. Global characterisation of the event and daily evolution

245 4.1 Maximum values of the event

Analysis of total event precipitation from 19 to 25 January 2020 shows that 90% of the stations recorded more than
40 mm. Of these, 37% recorded rainfall between 100 and 200 mm, while 22% exceeded 200 mm. The highest totals
occurred in northern Catalonia and in the Valencian Community (Fig. 3). Eleven stations, from Alicante to northern
Girona, recorded more than 400 mm, with a maximum of 527.5 mm at L'Orxa (Alicante; Table 3).

250



The large number of stations exceeding 200 mm confirms the exceptional character of the episode. For maximum wind gusts, 19 of the 140 stations exceeded 90 km h⁻¹ at some point during the event. The highest wind gusts were recorded in Valencia, with 108 km h⁻¹ on 19 January and 115 km h⁻¹ on the 20th, respectively (Table A1, in the Appendix). This same province also recorded the maximum wave height (8.44 m). Considering the three variables together, Valencia was the only province that reached the highest category for all three hazards. By contrast, in Granada only the lowest rainfall category was exceeded. Table 6 summarises the category reached by each variable in at least two stations in the province.

Note that the maximum rainfall tended to occur where coastal mountain ranges lie close to the shoreline, from Valencia to Catalonia, whereas the wave field, more directly controlled by the pressure gradient over the western Mediterranean, affected the entire coast. In the central and northern sectors, the easterly flow also blew almost perpendicularly to the coastline and the mountain ranges, enhancing orographic uplift and helping to explain the concentration of extreme rainfall in these areas.

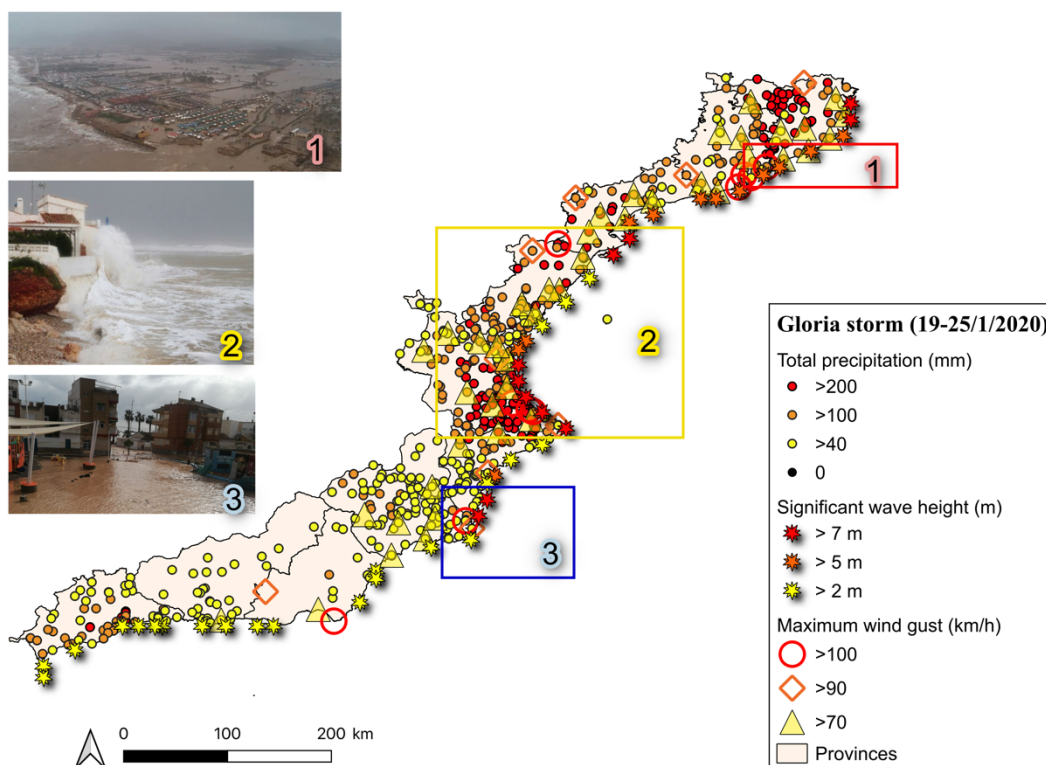




Figure 3: Map of the maximum thresholds exceeded at some point during the Gloria episode in the study area. Selected compound sub-events are highlighted with boxes and photographs: (1) multivariate in the Tordera River mouth; (2) spatially compounding on the coast of Valencia; and (3) temporally compound in los Alcázares.

270 **Table 3: Stations that recorded a total precipitation above 400 mm. *Coordinates are in decimal degrees (WGS84; EPSG:4326)**

Coordinates (lat, lon)*	Station name (altitude in m)	Province	Ptotal (19/1- 25/1)	P24h max (day)
38.84° N, 0.31° W	Lorxa (in L'Orxa) (270)	Alicante	527.5	266.5 (19)
42.29° N, 2.68° E	Albanyà-Lliurona (732)	Girona	515.2	208 (21)
39.00° N, 0.29° W	Barx-la Drova (372)	Valencia	471.5	273.6 (19)
38.81° N, 0.40° W	Gaianes (454)	Alicante	432.5	220.6 (19)
39.01° N, 0.30° W	Barx (340)	Valencia	432	242 (20)
41.81° N, 2.33° E	La Morera (in El Brull) (882)	Barcelona	424.5	236 (20)
38.74° N, 0.29° W	Benimassot (725)	Alicante	423	227.5 (20)
42.14° N, 2.53° E	Santa Pau-Sacot (609)	Girona	410.4	225 (21)
41.89° N, 2.43° E	Vilanova de Sau-El Tortades (818)	Barcelona	409.2	194.5 (21)
42.12° N, 2.63° E	Mieres (271)	Girona	408.7	150.5 (22)
42.26° N, 2.36° E	Sant Pau de Segúries-La Barquera (872)	Girona	403.5	220.5 (22)

4.2 Temporal evolution

Daily precipitation, maximum wind gust and significant wave height were analysed for the whole event (19-25
275 January). However, after 23 January, wave heights had fallen below the adopted thresholds, so the final two days
were relevant mainly for rainfall.

The first day of the event, 19 January, was characterised by values above the highest threshold for all three variables
(precipitation, wind gusts and wave height) in the province of Valencia. Notably, 277 mm were recorded in Barx



280 (Valencia), accompanied by a wind gust of 108 km h^{-1} . Significant wave heights over 7 m (with a maximum of 7.67 m) were observed offshore, particularly in front of the coasts of Valencia and Alicante, including the area near Jávea.

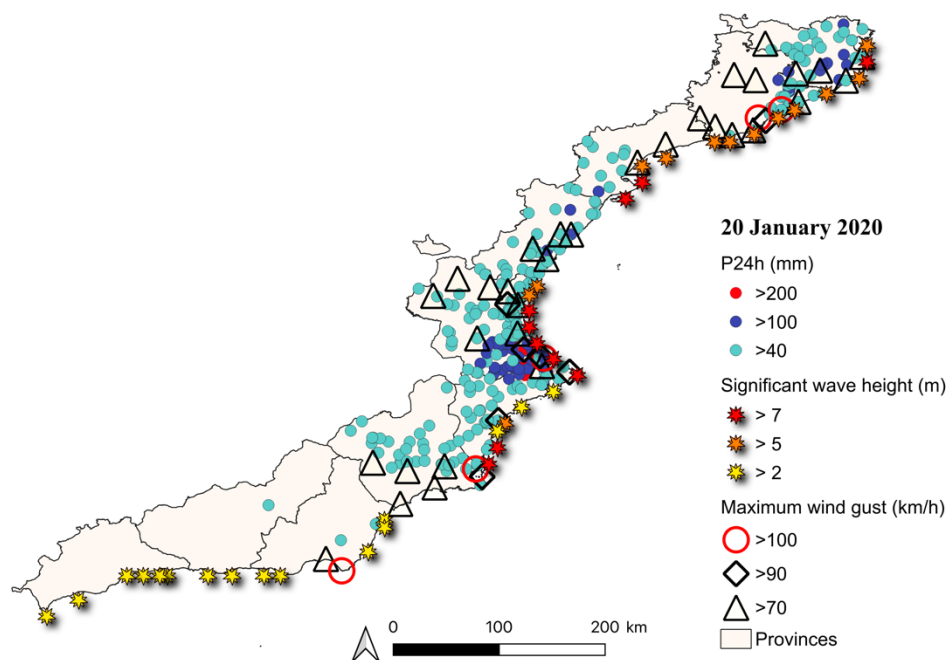


Figure 4: Stations where the wave height, maximum wind gusts and precipitation thresholds were exceeded on 20 January 2020.

285 **Appendix A contains maps for the other days of the event.**

On the 20th, the heaviest rainfall was again recorded in the provinces of Valencia and Alicante, with peaks of 242 mm in Barx and Xàtiva (Fig. 4). Wind gusts were more widespread and slightly stronger than the previous day, reaching a maximum of 115 km h^{-1} in Oliva (Valencia), followed by 104 km h^{-1} in San Javier (Murcia) and 103 km h^{-1} in the Fabra Observatory (Barcelona) and Cabo de Gata (Almería). Wave heights remained high, with the most extreme values again concentrated off the coasts of Valencia and Alicante, and locally in Girona and Tarragona. The highest recorded wave height was 10.1 m offshore from Jávea. On the 21st, the focus of maximum intensity shifted to the provinces of Barcelona and Girona, which recorded the highest across all three variables. Precipitation exceeded 200 mm at several locations, with a peak of 236 mm in El Brull (Barcelona). The maximum wind gust was 106 km h^{-1} , recorded at the Barcelona AEMET station. Significant wave heights above 5 m were observed

295



along the Catalan coast, particularly in Barcelona and Girona, with a maximum of 7.46 m in the northern coastal sector of Girona. On the 22nd, the intensity decreased compared to the previous day. Nevertheless, medium-level thresholds (level 2) were exceeded simultaneously for all three variables in the province of Girona, with the highest wave values still concentrated along the Catalan coast.

300

On the 23rd, the most notable rainfall occurred in the province of Málaga, with 202 mm recorded in Coín. Although heavy rainfall persisted in Málaga on 24 and 25 January, exceeding 100 mm on both days, no significant wind gusts or wave heights were recorded during this final phase of the event.

305 **5 Analysis of sub-events**

Among the many sub-events embedded within Storm Gloria, three of them were selected for probabilistic analysis (Table 4). Other processes that occurred during the episode are also relevant from a compound perspective. For example, the collapse of the road and railway bridges across the Tordera River illustrates a cascading sequence in which primary flood damage triggered secondary transport disruption. Likewise, the vulnerability of several
310 beaches had already been increased by earlier storms, which acted as a preconditioning factor before Gloria.

Table 4: Main characteristics of the selected compound sub-events and their estimated return periods

Type	Description	Selected data	Return period
<i>Multivariate (1)</i>	High rainfall intensity in the Tordera River basin + High sea waves	Weather stations in the Tordera River basin and CoExMed node in front of the mouth of the Tordera River.	85 years
<i>Spatially compounding (2)</i>	Maximum swell on the Jávea coast (Alicante) and heavy rainfall and flooding in the Júcar basin (Valencia), simultaneously.	Weather stations in the Júcar River basin and CoExMed node in front of Jávea.	72 years
<i>Temporally compounding (3)</i>	Three flood events between 11 September 2019 and 25 January 2020 in Los Alcázares (Murcia).	Weather stations in the Segura River basin and surrounding municipalities.	22 years



315 **5.1 Multivariate event: floods in the mouth of Tordera River**

5.1.1 Type

Multivariate: flooding caused by simultaneous fluvial overflow and severe wave conditions at the same site. In this case, intense rainfall in the Tordera River basin coincided with high-energy wave conditions near the river mouth, hindering drainage and aggravating flooding in the delta plain. The compound configuration does not modify the
320 marginal return period of each hazard separately; rather, it changes the joint probability and return period of their co-occurrence and associated impacts.

5.1.2 Description

Previous studies have already analysed the high complexity and risks of this area (e.g. Jiménez et al., 2018).
325 Extensive urban and infrastructure development along the coastline has made the region particularly vulnerable to extreme marine events which have already caused significant damage in the past. The delta at the mouth of the Tordera River (Fig. 1b) is retreating largely because of reduced sediment supply, and the adjacent beaches are therefore suffering intense erosion. Part of the area is occupied by campsites that are highly exposed to marine hazards, as the beach is the only protective barrier against sea storms. Moreover, the typical structures in these
330 campsites (tents, caravans, and lightweight bungalows) offer limited protection, increasing the vulnerability of occupants, particularly during holiday periods when occupancy is high. Additionally, there are currently no specific evacuation plans for campsites in the case of flood or storm warnings, further amplifying their potential impact. Also, the flood-prone area includes a major logistics hub and extensive agricultural land, both of which are also highly exposed. This combination of factors makes the area one of the most susceptible along the Catalan coast to
335 multivariate compound flood events (Sanuy et al., 2021).

5.1.3 Probabilistic analysis

The data used to create the time series in this multivariate scenario were obtained by considering all the rain stations within the Tordera River basin and the wave series from the CoExMed node closest to the river mouth (Fig. 5).



340

Figure 5: AEMET AWS (operative automatic weather stations, white circles) inside the Tordera River basin and surrounding area, and the node CoExMed nearest to the river mouth (red circle) (Map data © 2025 Google)

The maximum wave height and the maximum P24h registered in this subregion during the Gloria storm were 4.46
345 m and 225 mm respectively. From a univariate perspective, and by fitting a Generalized Pareto Distribution (GPD)
to the data, the estimated return periods for the wave storm and the rainstorm are approximately 60 years and 24
years, respectively.

To adopt a bivariate perspective, the joint return period of the co-occurring wave and rainfall extremes was
350 estimated. Assuming independence between the two variables, the joint return period would simply be the product
of their individual return periods, yielding $60 \times 24 = 1,440$ years. However, since dependence exists, this
relationship is modelled using copulas. Specifically, the dependence structure in the rainfall-conditioned analysis
(P24h₉₈, H_s) is captured using a survival BB7 copula with a Kendall's tau of 0.2, while the wave-conditioned
analysis (H_s_{99.5}, P24h) is modelled using a Tawn type 1 copula with a Kendall's tau of 0.1. Accounting for this
355 dependence, the resulting joint return period is estimated to be 85 years (Fig. 6).

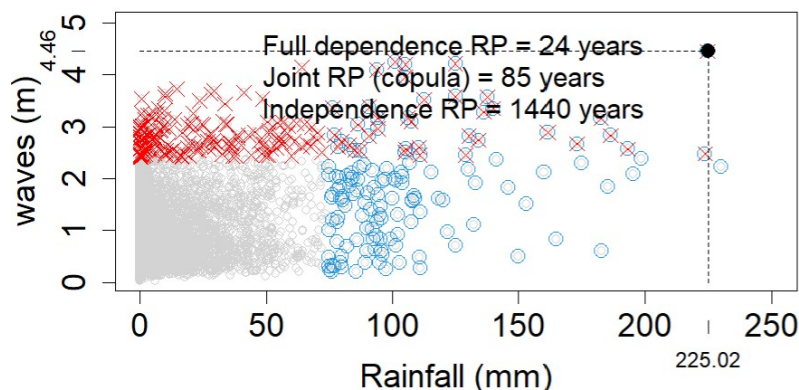


Figure 6: Estimated joint return period of the Gloria storm at Tordera River mouth, modelled as a multivariate event.

5.2 Spatially compounding inland–coastal event: heavy rainfall in the Júcar basin and high waves in the Gulf of Jávea

5.2.1 Type

Spatial compounding: it refers to situations in which the same hazard (or different hazards) occur simultaneously in different locations. These events can make emergency management and early-warning coordination more challenging when the affected areas fall under the responsibility of the same administration (e.g. civil protection authorities). While spatial compounding does not alter the return period of the hazard at each individual location, it does affect the return period of the event at the regional level. The event considered here combines the highest wave of the entire Gloria event, recorded off the coast of Jávea, with heavy rainfall and floods in the Júcar River basin (Fig. 7). Although impacts occurred in different areas, their simultaneity in the same autonomous community meant they had to be managed by the same administrations.

5.2.2 Description

The Valencian Community covers an area of 23,255 km² and includes a densely urbanised coastal margin intersected by numerous torrential, non-permanent streams (Fig. 1c). Within this setting, Jávea (68.59 km² in area, with 28,731 inhabitants) depends strongly on tourism as its main source of income. Its mountainous relief, the presence of ephemeral channels, and the intense occupation of the coastal fringe by housing, hotels, and other infrastructure make the municipality highly exposed to marine storms and flooding.

On 20 January, the Valencian coast experienced the most severe wave conditions of the event, with significant wave heights ranging from 7 to 10 m. The highest values were recorded off the coast of Alicante province,



380 particularly in front of Jávea, where severe damage occurred along the seafront promenade, and affected shops and
residences. A campsite in the area had to be evacuated, and additional impacts included road closures in other
sectors of the province, partly aggravated by concurrent snowfall inland. Also, most airports across the Valencian
Community were forced to suspend operations. To assess the extent of coastal inundation in Jávea and other
affected areas (including Dénia, Xàbia, south of Valencia, south of Castellón, the Ebro Delta, Maresme, Júcar–
385 Gandía, and Mallorca), the Copernicus Emergency Management Service was activated. Subsequent coastal-repair
measures approved by the Spanish administration exceeded EUR₂₀₂₂ 9 million.

5.2.3 Probabilistic analysis

The data series for this spatially compound scenario were obtained by considering all the precipitation records from
390 all the stations within the Júcar River basin and wave data from the CoExMed node located in the Gulf of Jávea
(Fig. 7).

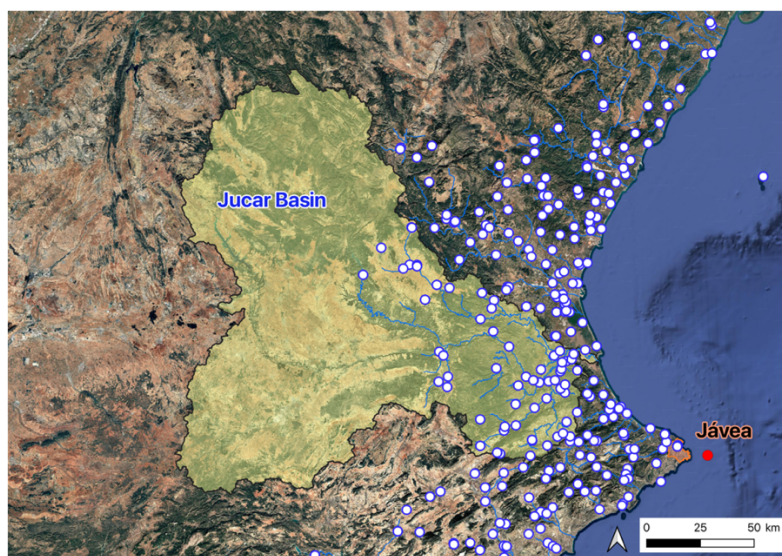


Figure 7: AEMET AWS (automatic weather stations, white circles) inside the Júcar River basin and surrounding area, and the node CoExMed located in the Gulf of Jávea (red circle) (Map data © 2025 Google)

395

During Storm Gloria, the maximum values recorded in this case-study domain were a significant wave height of 7 m and a daily precipitation total (P24h) of 274 mm. From a univariate perspective, the estimated return periods are about 1.5 years for the rainfall event. Thus, the wave conditions were exceptional, whereas rainfall totals of this order are not unusual within the climatology of the Júcar basin.

400



To capture the compound nature of the event, a bivariate analysis was used to estimate the joint return period of concurrent rainfall and wave extremes. Under an independence assumption, the product of the marginal return period would simply be the product of their individual return periods, yielding $100 \times 1.5 = 1,500$ years. However, since the variables are not independent, this relationship is modelled with copulas. Specifically, the dependence structure in the rainfall-conditioned analysis (P24h_98, Hs) is captured using a survival Tawn T2 copula with a Kendall's tau of 0.12, while the wave-conditioned analysis (Hs_99.5, P24h) is modelled using a Tawn type 1 copula with a Kendall's tau of 0.11. Accounting for this dependence, the resulting joint return period is estimated to be 72 years.

410 **5.3 Temporally compounding event: repeated impacts in Los Alcázares associated with temporally clustered episodes of heavy rainfall**

5.3.1 Type

Temporally compounding: a sequence of distinct events occurring within a relatively short period of time, such that recovery from one episode is incomplete before the next one occurs. The key issue here is not a change in the marginal return period of a single hazard, but the probability of repeated damaging conditions within a short time window. In the present case, Los Alcázares experienced repeated flood impacts between 19 September 2019 and 25 January 2020.

5.3.2 Description

420 Los Alcázares is a municipality in the Region of Murcia, located in the Segura River basin and extending along approximately 9 km of the Mar Menor coastline (Fig. 1d). In 2022, it had a resident population of 17,603 within an area of 19.82 km², although this figure increases markedly during the summer season due to tourism. The municipality is bordered to the south by the Rambla del Albuñón, while the historic urban centre is situated at the confluence of the Rambla de la Maraña and several smaller ravines (Fig. 8). This configuration favours a diffuse and spatially distributed flood response, with water entering the urban area through multiple drainage paths rather than a single well-defined channel. Although the immediate surroundings are relatively flat, the area is influenced by nearby medium-altitude mountain ranges with steep slopes, drained by numerous ephemeral streams flowing towards the Mar Menor. In this context, extensive urban development in flood-prone areas, the sealing and alteration of watercourses, and the presence of transport and utility infrastructure across drainage paths have contributed to high flood exposure and risk (Tragsatec and MITECO, 2020). Nearby municipalities such as San 430 Javier and San Pedro del Pinatar are affected by similar hydrometeorological conditions. The severity of this



435 exposure is reflected in the associated economic losses: between 1996 and 2020, the Consorcio de Compensación de Seguros (CCS) paid EUR₂₀₂₂ 45.7 million in compensation in Los Alcázares, placing it among the municipalities with the highest cumulative flood-related compensation losses in the Spanish Mediterranean region. The recurrence of the three flood events within such a short period significantly increased this local vulnerability, since the consequences of one episode had not yet been fully addressed when the next one occurred (Fig. 9).



Figure 8: Map of the municipality of Los Alcázares and neighbouring municipalities in Murcia mentioned in the text, showing rivers and AEMET AWS (automatic weather stations) (Map data © 2025 Google)

440

The first event, which occurred between 11 and 15 September 2019, was triggered by exceptionally intense rainfall across the Segura basin. Daily accumulations reached 257 mm in Molina de Segura on 12 September 2019, while San Javier recorded 321 mm in 24 hours on 13 September 2019. Total rainfall exceeded 450 mm in some parts of the region, and local short-duration intensities were also extreme, surpassing 30 mm in 10 minutes at some locations. Los Alcázares was among the municipalities most severely affected, largely as a result of the overflow of the Rambla del Albuji6n, which inundated large sectors of the town and caused serious damage to infrastructure, including the Town Hall (Fig. 9). The magnitude of the impacts led to the official declaration of the municipality as a *Zona afectada gravemente por una emergencia de protecci6n civil* (area seriously affected by a civil protection emergency). For this episode alone, the CCS paid more than EUR₂₀₂₂ 24 million in Los Alcázares, accounting for 74% of the total compensation disbursed in the municipality between 1996 and 2020. By contrast, its location on

450



the shores of the Mar Menor, which is separated from the open Mediterranean by the narrow barrier of La Manga, explains the absence of documented damage associated with storm surge, including during Storm Gloria.



(a)



(b)

Figure 9: Floods in Los Alcázares: (a) September 2019, during the DANA event (source: Confederación Hidrográfica del Segura); and (b) January 2020 (source: Government of the Region of Murcia)

455

Just under three months later, on 2–3 December 2019, the area was affected by a second episode of heavy rainfall. The highest daily accumulation, 145 mm, was recorded in Benizar, in the northern sector of the Segura River basin, while San Javier registered 115 mm in 24 hours. The event caused widespread flooding of major roads and led to the evacuation of around 100 residents from the most exposed areas. Although shorter and less severe than the
460 September episode, this second event compounded previous losses and exposed the fragility of infrastructure that was still under repair. In Los Alcázares, CCS compensation for this flood exceeded EUR₂₀₂₂ 400,000.

The third episode was Gloria, which affected the region mainly between 20 and 21 January 2020. On 22 January, the Municipal Emergency Plan was activated at Level 1 in both San Pedro del Pinatar and San Javier (neighbouring
465 municipalities to Los Alcázares), reflecting the seriousness of the situation. Numerous flooding incidents were reported, and CCS estimated the associated losses at around EUR₂₀₂₂ 26,000. However, the distinctive feature of this event was not the scale of the material damage, which was comparatively moderate, but the strength of the social response. Dissatisfaction with the authorities' management generated numerous citizen complaints and culminated in a public demonstration in Los Alcázares on 26 January.

470

Taken together, these three episodes illustrate not only the high hydrometeorological hazard affecting the region, but also the cumulative character of vulnerability. Recurrent impacts within a short period, incomplete recovery



processes, and perceived limitations in institutional response amplified both the economic and the social consequences of the events.

475

5.3.3 Probabilistic analysis

For this case, the analysis uses daily precipitation records from the official Segura basin network as a proxy for the regional hydrometeorological forcing associated with the repeated impacts in Los Alcázares (Fig. 9). The resulting return period therefore refers to a sequence of basin-scale rainfall extremes, not to the recurrence of flooding losses in Los Alcázares itself.

480

During Storm Gloria, the Segura River basin recorded a maximum 24-hour precipitation total (P24h) of 145 mm. As noted above, this event occurred under already exceptional antecedent wetness, with 115 mm accumulated over the previous month and 257 mm over the preceding three months, highlighting that Gloria formed part of a short sequence of unusually intense rainfall episodes. In this case, the key issue is not the magnitude of an individual storm, but the temporal clustering of extremes. Within less than five months, the basin experienced three high-magnitude events, one of which exceeded 200 mm. This recurrence appears only once in the 43-year observational record, corresponding to an empirical return period of approximately 22 years. Although this estimate provides a useful reference for risk assessment, it should be interpreted with caution given the limited length of the observational record and the uncertainty inherent in empirical recurrence estimates for clustered extreme events.

485

490

6 Main damage and economic compensation

6.1 Impacts

Storm Gloria caused extensive damage across a wide area. According to CCS data, the event affected 770 municipalities, representing 46% of all municipalities in the analysed provinces and 82% of those located along the coast (Table 5). The event was also associated with 13 fatalities and 4 missing people. Among the fatal cases for which location was identified, two occurred in the province of Tarragona, one in Girona, and one in Barcelona, all in Catalonia; two occurred in Valencia, in the Valencian Community; and two in Almería, in Andalusia. Of these eight identified victims, seven were men. The reported causes of death were mainly related to the adverse maritime conditions (2 cases), hypothermia (3 cases), and flooding (3 cases, including 2 people trapped in vehicles).

495

500



Table 5: Number of municipalities affected by flooding, storm surge, or TCA, by coastal provinces in every autonomous community and for the study area as a whole. *In the total figure for each region, each municipality is counted only once, even if it has been affected by one, two or three hazards. The total number of municipalities in each province is provided in Appendix A.

	Catalan prov.	Valencian prov.	Murcia prov.	Andalucia prov.	Total
Floods	422	224	15	31	692
Sea storm	55	45	2	0	102
TCA	194	56	4	2	256
Total*	474	249	15	32	770

505

The storm severely affected large sections of the Mediterranean coastline, particularly in Catalonia and the Valencian Community, where extensive beach erosion and substantial damage to coastal infrastructure, including promenades and harbours, were reported. In urban areas, the overflow of rivers and streams caused widespread flooding, affecting vehicles, residential buildings, commercial premises, industrial facilities, and hotels. Strong winds, especially in Barcelona, caused further damage to urban furniture and other public assets.

Transport networks were also seriously disrupted, as several railway lines and roads were cut off by flooding, landslides, fallen trees, or snow accumulation. In Catalonia, four bridges collapsed, including the railway and motorway bridges over the Tordera River. Rail services were not fully restored until ten months later. Airports in the Valencian Community and Andalusia also experienced operational disturbances.

The agricultural and fisheries sectors likewise sustained considerable losses. In the Ebro Delta, rice crops were heavily affected, while in Níjar (Almería), numerous greenhouses suffered severe damage. The Union of Small Farmers and Ranchers estimated total agricultural losses in Spain at EUR₂₀₂₂ 24.12 million. Fishing activity was completely suspended during the storm and remained hindered for more than a week afterwards due to sediment and debris transported by rivers. In addition, boats, fishing gear, and offshore fattening cages suffered significant damage; in the latter, located off l’Ametlla de Mar (Tarragona), thousands of tunas died.

From an ecological perspective, the storm had substantial impacts on several natural environments, including the Ebro Delta (Catalonia) and l’Albufera of Valencia. Particularly severe damage was reported in *Posidonia*

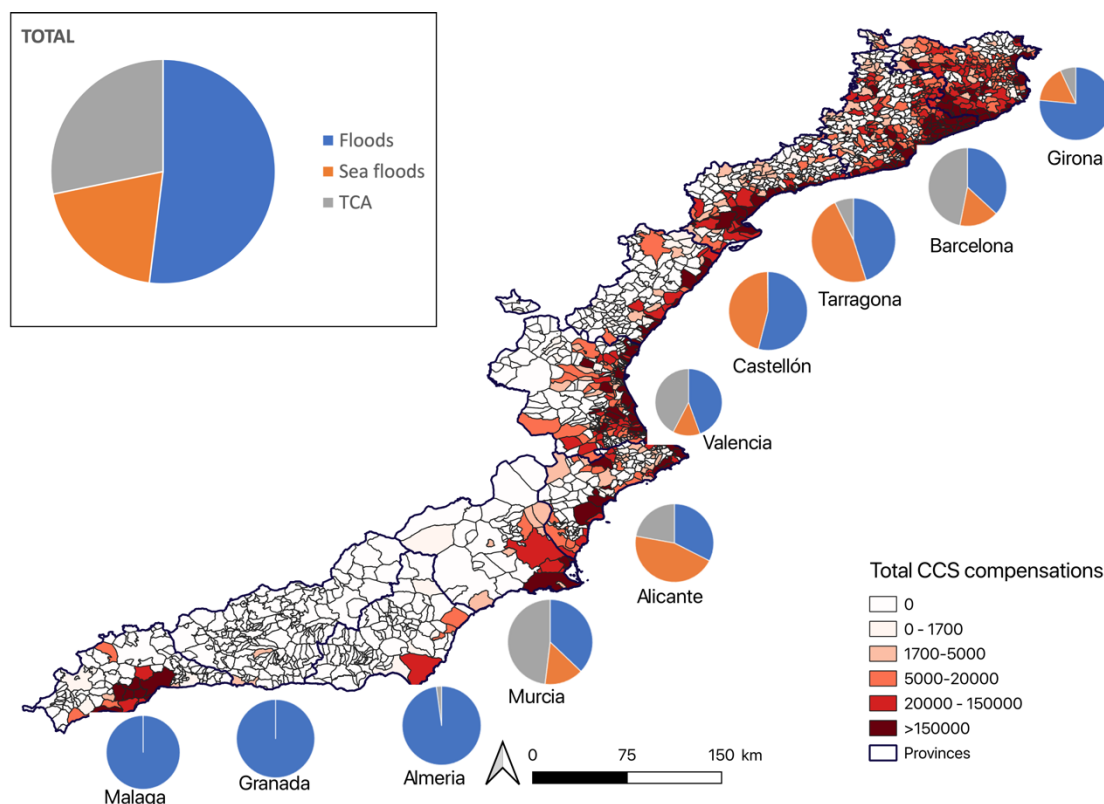


530 *oceanica* meadows, which were strongly affected by the marine storm, while intense winds also caused widespread tree uprooting. At the same time, some positive effects were identified, such as the regeneration of the Tordera delta through sediment input and the recharge of aquifers and reservoirs. Daily life was also seriously disrupted, with school closures, interruptions to electricity and drinking water supply, and damage to collectors, water treatment plants, and sewage systems in multiple localities. Beyond these direct effects, the event generated significant indirect impacts, including travel delays and the temporary suspension of economic activity. Intangible damage should likewise be acknowledged, following the classifications proposed by Petrucci and Llasat (2013) and Messner and Meyer (2006), particularly anxiety and stress among affected populations.

535

6.2 Compensation

The total amount of compensation paid across the study area reached EUR₂₀₂₂ 204 million, of which EUR₂₀₂₂ 106.5 million was associated with flooding, EUR₂₀₂₂ 40.3 million with sea storms, and EUR₂₀₂₂ 57.2 million with TCA. Figure 10 shows the distribution of these payments by hazard type: 52% corresponded to floods, 28% to TCA, and 540 20% to sea storms. A similar pattern is observed when only coastal municipalities are considered. In these municipalities, 43% of compensation was associated with floods, while TCA and sea storms each accounted for 29%.



545 **Figure 10: Map of the sum of flood, sea storm and TCA compensation with indication of the distribution of quantities according to the causes**

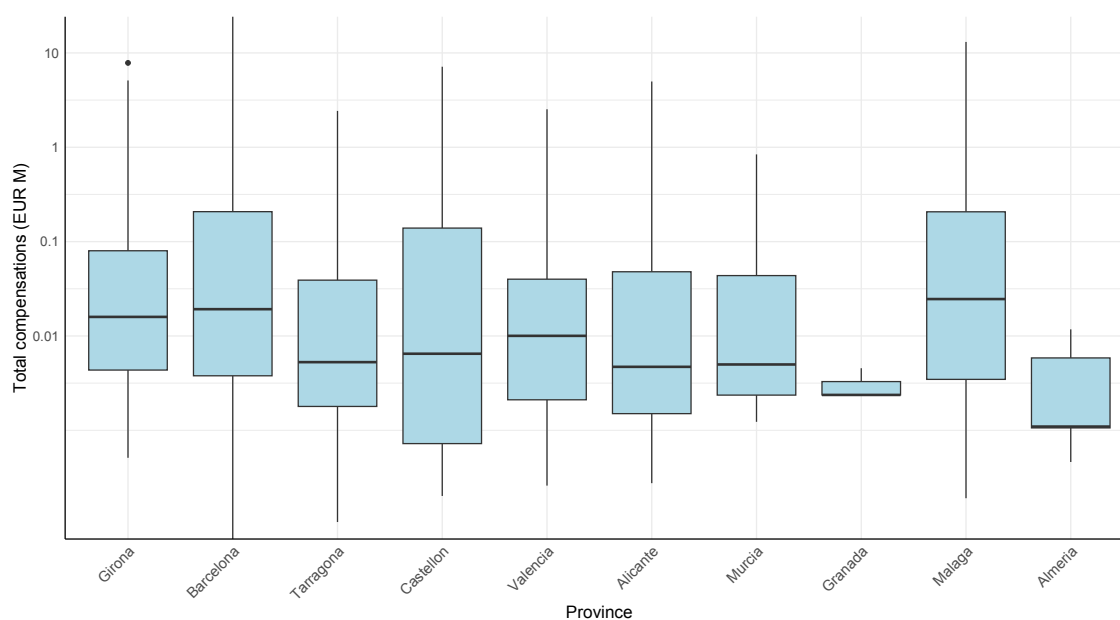
In most provinces, the largest share of compensation was associated with flooding, either alone or in combination with sea storms. This pattern was particularly marked in the Andalusian provinces, where compensation was almost entirely flood-related: 100% in Granada, 99.9% in Málaga, and 98% in Almería, with only 0.03% and 2%, respectively, attributable to TCA. Given that rainfall totals were lower in the southern sector and that GDP levels were not among the highest, the comparatively large flood-related compensation suggests a stronger role of exposure, particularly the occupation of flood-prone areas, and the high value of the insured assets, given that the region is home to some luxury residences.

555

At municipal scale, the distribution of impacts also highlights the complexity of hazard interactions. More than half of the municipalities at the provincial level were affected exclusively by floods, while 18% experienced both floods and TCA, and 5% were affected simultaneously by all three hazards. Among coastal municipalities, 20% were affected solely by floods, 42% by the combination of floods and sea storms, 7% by floods and TCA, and 29% by

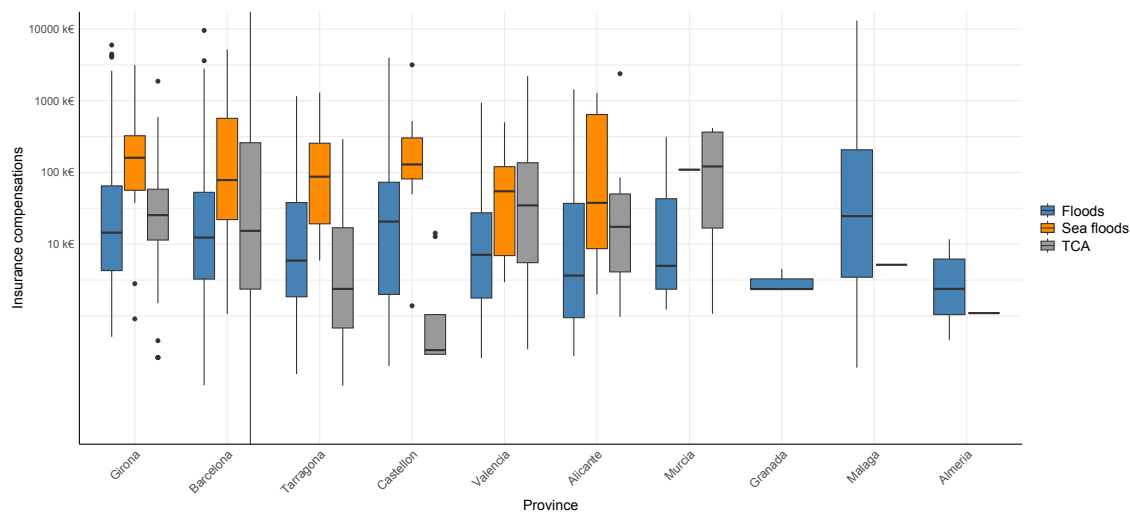


560 all three causes. The municipalities that received the highest total compensation, considering the combined effect
of the three hazards, were Barcelona (EUR₂₀₂₂ 24 million), followed by Málaga (EUR₂₀₂₂ 13 million) and Malgrat
de Mar (EUR₂₀₂₂ 10 million). In the case of Malgrat de Mar, this result is unsurprising given its location near the
mouth of the Tordera River. For Barcelona, the high compensation is consistent with the intensity of rainfall, the
large exposed population, and the high value of exposed assets. Málaga, however, reflects a different configuration:
565 although average GDP is lower, the presence of numerous high-value second homes increased insured losses
substantially. Overall, these results illustrate the complexity involved in interpreting impact patterns, which depend
not only on hazard intensity but also on the spatial distribution and value of exposed elements.



570 **Figure 11: Distribution of compensation paid to municipalities within each province. The y-axis is shown on a log₁₀ scale with values expressed in EUR₂₀₂₂ million.**

Figure 11 further shows that Málaga has the highest compensation values per municipality, as well as greater dispersion of values than neighbouring regions. Granada shows the lowest number of municipalities receiving compensation, followed by Almería; both with a concentration of municipalities with low compensation values.
575 This pattern reinforces the complexity of the hazard–impact relationship, which cannot be explained by hazard intensity alone but must also consider multiple factors related to exposure and vulnerability. In the same vein, Fig. 12 indicates that no single spatial pattern explains the distribution of compensation by hazard factors.



580 **Figure 12: Distribution of compensation paid to each municipality located in each province, by hazard. In the case of Murcia, only two municipalities received compensation for sea floods, while in the Andalusian provinces, compensation was only related to floods, except in Almería and Málaga, where one municipality in each province received compensation for TCA.**

Finally, the 10 provinces were classified according to both hazard intensity and compensation paid. Hazard classification was based on the *hazard level categories* defined in Section 4.1, considering in each province the maximum threshold exceeded. Compensation values were classified using the 33rd and 66th percentiles of each series, which were applied separately to each type of compensation. Table 6 presents the resulting hazard and compensation categories using numerical class labels. Hazard categories are indicated as H1, H2 and H3, while compensation categories are indicated as C1, C2 and C3, corresponding respectively to low, intermediate and high levels. For each province and hazard type, the *hazard category* was then compared with the corresponding *compensation category*. Overall, a broadly consistent relationship emerges: provinces with the highest CCS payments generally correspond to category H3 in the hazard classification, indicating that at least two measurement points exceeded the highest threshold. One notable exception is Barcelona, where compensation related to sea storms reached the highest category, C3, even though the corresponding hazard was not classified at that level. This result, however, coincided with maximum-category values for the other two hazards and their associated CCS payments. Conversely, some provinces, such as Tarragona and Valencia, reached the highest hazard category without showing equally high compensation values. These discrepancies may reflect contextual factors that limited the resulting damage, including lower exposure or vulnerability in the affected areas.

585

590

595



600 **Table 6: Hazard categories attained in each province according to the maximum threshold exceeded at a minimum of two stations or one station and one SIMAR point, and total compensation paid by hazard type and province, expressed in EUR₂₀₂₂ million (M). Ptotal: total precipitation, Wmax: maximum wind gust, SH: sea wave height; CCS-Floods: compensation related to flooding; CCS-Sea floods: compensation related to sea floods; CCS-TCA: compensation related to wind-related claims.**

Province	Ptotal	CCS-Floods (M)	SH	CCS-Sea floods (M)	Wmax	CCS-TCA (M)
Girona	H3	35.13 (C3)	H3	7.59 (C3)	H1	3.20 (C2)
Barcelona	H3	33.84 (C3)	H2	14.89 (C3)	H3	43.04 (C3)
Tarragona	H3	5.01 (C2)	H3	5.29 (C2)	H1	0.81 (C1)
Castellón	H3	6.16 (C2)	H1	5.23 (C2)	H2	0.03 (C1)
Valencia	H3	6.98 (C3)	H3	2.07 (C2)	H3	6.66 (C2)
Alicante	H3	3.81 (C2)	H3	5.32 (C2)	H2	2.60 (C2)
Murcia	H2	0.63 (C1)	H1	0.25 (C1)	H2	0.81 (C1)
Almería	H1	0.05 (C1)	H1	-	H2	0.001 (C1)
Granada	H1	0.009 (C1)	H1	-	-	-
Málaga	H3	14.93 (C3)	H1	-	-	0.005 (C1)

605 7 Conclusions

Storm Gloria, which affected the Mediterranean coast of Spain (174 municipalities, 1,609 km of coastline and 12,167 km²) between 19 and 25 January 2020, was characterised by an exceptional combination of intense rainfall, flash floods, floods, snowfalls, hailstorms, very strong wind gusts, and record-breaking wave heights. The concurrence of these meteorological and maritime extremes makes Gloria a paradigmatic compound event, in which interacting drivers amplified impacts well beyond those that would be expected from each hazard in isolation. The episode caused severe economic and social disruption across the region, highlighting the need for an integrated, regional-scale perspective to better understand its dynamics, assess the associated risks, and inform effective coastal management strategies.

615 During the Gloria event, precipitation was widespread, with the highest accumulations recorded in the provinces of Girona (northern part), and Valencia and Alicante (central part), exceeding 500 mm in numerous stations (maximum of 527.5 mm). Maximum wind gusts and significant wave heights broadly followed a similar spatial pattern, although wave heights were comparatively lower along the Andalusian coast (southern part). The event reached its peak between 19 and 21 January, when several stations recorded daily precipitation totals exceeding
 620 200 mm (maximum, 266.5 mm/24h) and the maximum values for all three variables (wind gust of 115 km h⁻¹,



maximum wave height 8.44 m) were recorded on 20 January. From 22 January onwards, the intensity gradually declined: wind gusts rarely exceeded 70 km h^{-1} and significant wave heights along the Catalan coast fell below 4 m after 23 January. However, heavy rainfall exceeding 100 mm persisted in Málaga (southern part) on 24 and 25 January, after wind and wave activity had already subsided in most other areas. To characterise the event from a risk perspective, three daily thresholds were defined for each variable (precipitation, maximum wind gust, maximum wave height). This allowed each weather station to be classified into three intensity categories and enabled the analysis of daily trends and extreme values throughout the entire event. The highest intensity category, corresponding to the third threshold, was exceeded simultaneously for all three variables at several sites in Castellón and Valencia. Some stations in Girona, Barcelona, Alicante, and Murcia exceeded the highest threshold for two variables, further illustrating both the spatial heterogeneity and the compound nature of the event.

The event was further examined in detail to identify specific situations, or sub-events, corresponding to the compound-event typologies proposed by Zscheischler et al. (2020). A representative example is the flooding of the Tordera River basin, located between the provinces of Barcelona and Girona. In this case, flooding resulted from the simultaneous occurrence of intense precipitation within the basin and elevated wave heights near the river mouth, which hindered drainage into the sea. This sub-event was therefore classified as multivariate. A probabilistic assessment of the joint occurrence of extreme rainfall and high-wave conditions yielded a return period of 85 years, highlighting the exceptional character of the episode, particularly regarding the marine component. In this sub-event, the high exposure of transport and communication infrastructure played a decisive role, leading to severe and prolonged disruption to daily life for the local population. Vulnerability was further increased by the high concentration of campsites in the affected area. Together with territorial features, such as a complex network of ephemeral streams, these factors make the area especially prone to flooding and to the cascading effects associated with compound hazards. The recovery process was correspondingly complex and prolonged, largely because responsibility for the damaged infrastructure was distributed across multiple administrative levels (local, regional, and national). Six years later, work is still underway in the Tordera Delta to try to implement a combination of Nature-based Solutions, land reclassification and structural measures.

A further relevant case is the municipality of Los Alcázares, in the region of Murcia, which experienced flooding for the third time within a five-month period and therefore fits the definition of a temporally compounding event. The area was severely affected in September 2019 and flooded again in December 2019, when streets in the municipality were once more inundated. As a result, the January 2020 event had a stronger social impact, not



655 primarily because of its intrinsic severity, but because it occurred in a context of cumulative damage and incomplete recovery from the previous floods. A probabilistic analysis indicates a return period of approximately 22 years for the occurrence of three rainfall events exceeding 100 mm within five months in the Segura River basin. In this area, high exposure is largely explained by urban development in flood-prone zones, which substantially increases flood risk. At the same time, the comparatively moderate impacts of the January 2020 episode allowed for a more effective municipal response. In addition, the Central Administration activated an existing recovery mechanism, making it possible to address the damage caused by this event under the provisions of the 2019 Floods Decree and thereby facilitating access to compensation and support.

660

The spatially compounding type is illustrated by the simultaneous occurrence of heavy rainfall in the Júcar basin and exceptional wave heights in the Gulf of Jávea, in the province of Alicante. Record-breaking wave heights were observed in this sector, with probabilistic analyses indicating a return period of approximately 100 years for wave height alone and 72 years for the combined inland–coastal event. The high levels of urbanisation and tourism in the area contribute substantially to its exposure to coastal hazards. Coastal infrastructure sustained severe damage, prompting the activation of the Copernicus Emergency Management Service to map marine inundation in Jávea. The complexity of the situation was further increased by the simultaneous occurrence of several high-risk scenarios within a relatively limited geographical area.

670 When accumulated rainfall is analysed at station scale, several locations show totals associated with high return periods, further reflecting the exceptional nature of the episode in specific areas. For example, the 328 mm recorded in Xàtiva (Valencia) corresponds to an estimated return period of approximately 88 years, indicating a rare event (AEMET, 2020b). By contrast, even higher totals at other stations were associated with shorter return periods. In Barx (Valencia), for instance, 433 mm were recorded, yet the estimated return period is only 10 years. This suggests that, despite the exceptional absolute magnitude of the rainfall, such accumulations are comparatively more frequent in that area.

680 Overall, the simultaneous occurrence of multiple hazards triggered the activation of numerous emergency response services. However, most of the emergency management during the event was led by municipal administrations, given the localised nature of the initial impacts. In practice, the storm affected many municipalities in rapid succession, placing substantial pressure on local response capacity. During the post-event phase, the central



government assumed a more prominent role, particularly in recovery operations, in view of the extent and severity of the damage across the eastern Mediterranean coast.

685 In terms of impacts, the most substantial damage was concentrated in beaches, port facilities and critical
infrastructures near the sea. Severe coastal erosion and the widespread destruction of beach infrastructure generated
major social disruption, with long-lasting consequences for key economic sectors such as tourism. Ports also
sustained considerable economic losses and required reconstruction efforts extending over more than three years.
In addition, damage was reported in other sectors, including agriculture, transport, and communication
690 infrastructure. Another cascading event was the destruction of the railway and motorway bridges over the Tordera
River, which run parallel to the sea, and which did not become operational again until five months later.

From an economic perspective, the comparison between compensation levels and the severity of the meteorological
extremes reveals a broadly consistent relationship: the highest compensation values generally coincide with
695 meteorological variables reaching the highest intensity category. However, the converse does not always apply,
since extreme rainfall, wind gusts, or wave heights do not necessarily translate into equally high economic losses.
This indicates that the final economic impact of extreme events is also strongly conditioned by factors such as
exposure, vulnerability, insurance coverage, and reporting practices. The episode also placed substantial pressure
on institutional response mechanisms, particularly the CCS, which faced major difficulties in processing claims
700 due to the residual burden of previous flood events in late 2019. In several cases, recovery was complex and
prolonged, a situation that was later aggravated by the onset of the COVID-19 pandemic and the associated
restrictions from March 2020 onwards.

The storm also caused significant damage to coastal ecosystems, including *Posidonia* meadows and
705 environmentally sensitive areas such as the Ebro Delta, thereby amplifying its social and ecological consequences.
The widespread accumulation of debris, including logs, vegetation, and waste, along beaches and riverbanks led
several municipalities to launch community-based clean-up campaigns, actively involving citizens in
environmental restoration efforts. At the same time, in some areas the storm also produced beneficial ecological
effects, contributing to the natural regeneration of degraded deltaic habitats and creating new refuge areas in rivers
710 and lakes through the redistribution of organic material.



The study has shown how compound events like Storm Gloria can be characterised in multiple dimensions, including hazard type, spatial extent, temporal evolution, and administrative scale. In compound events, these dimensions often overlap, generating complex situations where conventional response protocols may prove
715 insufficient, given the need to manage multiple hazards and levels of governance simultaneously. This underscores the need for flexible and robust decision support tools capable of supporting effective response planning in complex situations without compromising scientific rigour. At the same time, improving our understanding of compound events remains a key priority. In this regard, the study contributes by proposing a structured methodology for classifying sub-events and applying a severity scale to assess the intensity of the associated hazards. This detailed
720 analysis of a single event also highlights several challenges and opportunities for advancing compound-event research. One important line of development is the application of probabilistic methods to assess the joint occurrence of multiple hydrometeorological hazards, such as heavy rainfall and high wave activity. These approaches offer considerable potential for improving regional risk assessment, particularly by redefining return periods in terms of hazard combinations rather than treating each driver independently.

725

The study also demonstrates the importance of an interdisciplinary perspective, integrating expertise from meteorology, hydrology, coastal engineering, and risk management to address the complexity of compound events more comprehensively. More broadly, it highlights the value of analysing spatially extensive yet climatically and socio-economically coherent regions, such as the Mediterranean coast of the Iberian Peninsula, where shared
730 characteristics provide a consistent framework for comparative analysis. Ultimately, studies of this kind provide a valuable basis for developing methodologies that can inform planning and resource allocation in anticipation of future compound events. Progress in this direction may contribute to the design of operational tools that support risk-informed decision-making and strengthen emergency preparedness across multiple administrative levels.

Code and data availability

735 All meteorological data used come from the Spanish Meteorological Agency (AEMET, Agencia Estatal de Meteorología, link: https://www.aemet.es/en/datos_abiertos); sea-wave data, from Puertos del Estado (<https://www.puertos.es/en/services/oceanography>); data on financial compensation come from the Insurance Compensation Consortium (<https://www.conorseguros.es/en/>). Data on flood episodes come from INUNGAMA and can be downloaded from <https://agora.ub.edu>.



740 **Author contributions**

MLB conceptualised the study and conducted the research. MA designed and carried out the probabilistic analysis of sub-events and provided CoExMed and SIMAR data. MLB was responsible for the data curation, analysis and maps preparation. JAJ evaluated and discussed the results. MLB, MCL and RM prepared the manuscript with contributions from all co-authors, including the revised versions.

745 **Competing interests**

The authors have the following competing interests: At least one of the (co-)authors is a member of the editorial board of Natural Hazards and Earth System Sciences

Disclaimer

750 Copernicus Publications remains neutral with regard to jurisdictional claims made in the text, published maps, institutional affiliations, or any other geographical representation in this paper. While Copernicus Publications makes every effort to include appropriate place names, the final responsibility lies with the authors. Views expressed in the text are those of the authors and do not necessarily reflect the views of the publisher.

Acknowledgements

755 We would like to thank Puertos del Estado and AEMET for providing the wave data (SIMAR database) and meteorological data used in this study, respectively, and CCS, La Vanguardia, and other press databases for the information on impacts. One of the co-authors, Raül Marcos-Matamoros, is a Serra Hünter fellow.

Financial support

760 This work has been supported by the Spanish Project C3RiskMed (grant no. PID2020-113638RB-C22, AEI/10.13039/501100011033) and INUND-IA project (RDI001/24/000013 financed by the Catalan Water Agency).

References

AEMET: Informe sobre borrascas y Gloria, <https://www.aemet.es/ca/conocerlas/borrascas/2019-2020> (last access: 25 March 2025), 2025.



- AEMET: Informe de episodio de precipitaciones intensas en Málaga el día 25 de enero de 2020, 2020a.
- 765 AEMET: Informe de episodio meteorológico de temporal invernal (fecha de elaboración: 27/01/2020), 2020b.
- Amaro, J., Gayà, M., Aran, M., and Llasat, M. C.: Preliminary results of the Social Impact Research Group of MEDEX: The request database (2000–2002) of two Meteorological Services, *Nat. Hazards Earth Syst. Sci.*, 10, 2643–2652, <https://doi.org/10.5194/nhess-10-2643-2010>, 2010.
- Amores, A., Marcos, M., Carrió, D. S., and Gómez-Pujol, L.: Coastal impacts of Storm Gloria (January 2020) over the north-
770 western Mediterranean, *Nat. Hazards Earth Syst. Sci.*, 20, 1955–1968, <https://doi.org/10.5194/nhess-20-1955-2020>, 2020.
- Bevacqua, E., Maraun, D., Vousdoukas, M. I., Voukouvalas, E., Vrac, M., Mentaschi, L., and Widmann, M.: Higher probability of compound flooding from precipitation and storm surge in Europe under anthropogenic climate change, *Science Advances*, 5, eaaw5531, <https://doi.org/10.1126/sciadv.aaw5531>, 2019.
- Bolaños-Sánchez, R., Sánchez-Arcilla, A., Espino, M., and Grifoll, M.: Analysis and comparison of coupled and uncoupled
775 simulations with the COAWST model during the Gloria Storm (January 2020) in the northwestern Mediterranean Sea. *Environmental Modelling & Software*, 165, 105766, 2023.
- Canals, M. and Miranda, J.: Sobre el temporal Gloria (19-23.01.20), els seus efectes sobre el país i el que se'n deriva, Report de Resposta Ràpida, edited by: Canals Artigas, M. and Miranda i Canals, J., 201 pp., 2020.
- Coles, S.G. and Tawn, J.A.: Modelling extreme multivariate events, *J. R. Statist. Soc.*, B 53, 377–392, 1991.
- 780 Coles, S., Heffernan, J. and Tawn, J.: Dependence Measures for Extreme Value Analyses, *Extremes* 2, 339–365, <https://doi.org/10.1023/A:1009963131610>, 1999.
- Comisionado del Gobierno frente al Reto Demográfico (CGRD): Diagnóstico: Estrategia Nacional frente al Reto Demográfico. Eje Efectos de la Población Flotante, Ministerio para la Transición Ecológica y el Reto Demográfico, [https://www.miteco.gob.es/content/dam/mitesco/es/reto-demografico/temas/analisis-](https://www.miteco.gob.es/content/dam/mitesco/es/reto-demografico/temas/analisis-cartografia/diagnostico_eje_flotante_tcm30-517771.pdf)
785 [cartografia/diagnostico_eje_flotante_tcm30-517771.pdf](https://www.miteco.gob.es/content/dam/mitesco/es/reto-demografico/temas/analisis-cartografia/diagnostico_eje_flotante_tcm30-517771.pdf) (last access: 25 September 2025), 2019.
- Cortès, M., Turco, M., Llasat-Botija, M., and Carmen Llasat, M.: The relationship between precipitation and insurance data for floods in a Mediterranean region (northeast Spain), *Nat. Hazards Earth Syst. Sci.*, 18, 857–868, <https://doi.org/10.5194/nhess-18-857-2018>, 2018.
- Cortès, M., Turco, M., Ward, P., Sánchez-Espigares, J. A., Alfieri, L., and Llasat, M. C.: Changes in flood damage with global
790 warming on the eastern coast of Spain, *Nat. Hazards Earth Syst. Sci.*, 19, 2855–2877, <https://doi.org/10.5194/nhess-19-2855-2019>, 2019.
- De Alfonso, M., Lin-Ye, J., García-Valdecasas, JM., Pérez-Rubio, S., Luna, MY., Santos-Muñoz, D., Ruiz, MI., Pérez-Gómez, B and Álvarez-Fanjul, E.: Storm Gloria: Sea State Evolution Based on in situ Measurements and Modeled Data and Its Impact on Extreme Values, *Front. Mar. Sci.*, 8: 646873, <https://doi.org/10.3389/fmars.2021.646873>, 2021.
- 795 Del Río, L., Plomaritis, T. A., Benavente, J., Valladares, M., and Ribera, P.: Establishing storm thresholds for the Spanish Gulf of Cádiz coast, *Geomorphology*, 143–144, 13–23, <https://doi.org/10.1016/j.geomorph.2011.04.048>, 2012.



- Genest, C., and Favre, A. C.: Everything you always wanted to know about copula modeling but were afraid to ask, *Journal of hydrologic engineering*, 12, 4, 347-368, 2007.
- González, M. (coord.): *El temporal Gloria (19-23/01/2020): els efectes dels processos geològics sobre el territori*, Institut Cartogràfic i Geològic de Catalunya, Barcelona, 122 pp., 2020.
- IPCC: *Managing the Risks of Extreme Events and Disasters to Advance Climate Change Adaptation. A Special Report of Working Groups I and II of the Intergovernmental Panel on Climate Change (IPCC)*, Cambridge University Press, Cambridge, UK, and New York, NY, USA, 109–230, 2012.
- Jiménez, J. A., Sanuy, M., Ballesteros, C., and Valdemoro, H. I.: The Tordera Delta, a hotspot to storm impacts in the coast northwards of Barcelona (NW Mediterranean), *Coastal Engineering*, 134, 148–158, <https://doi.org/10.1016/j.coastaleng.2017.08.012>, 2018.
- Leeding, R., Riboldi, J., and Messori, G.: *Weather and Climate Extremes*, Volume 39, <https://doi.org/10.1016/j.wace.2022.100524>, 2022.
- Leonard, M., Westra, S., Phatak, A., Lambert, M., van den Hurk, B., McInnes, K., Risbey, J., Schuster, S., Jakob, D., and Stafford-Smith, M.: A compound event framework for understanding extreme impacts, In *Wiley Interdisciplinary Reviews: Climate Change*, Vol. 5, Issue 1, pp. 113–128, Wiley-Blackwell, <https://doi.org/10.1002/wcc.252>, 2014.
- Llasat, M.C., Llasat-Botija, M., Pardo, E., and Esbrí, L.: Informe tècnic de l'episodi d'inundacions del 19 a 23 de gener de 2020, Informe d'Estudi Projecte Agora 22, Universitat de Barcelona, <https://agora.ub.edu/portal-historic/> (last access: 13 February 2026), 2023.
- Luján López, A.: *Las siniestralidades de Gloria*, *Conorseguros Revista digital*, 1–14, 2022.
- MedECC: Summary for Policymakers, In: *Climate and Environmental Coastal Risks in the Mediterranean*. [Djoundourian, S., Lionello, P., Llasat, M.C., Guiot, J., Cramer, W., Driouech, F., Gattacceca, J.C., Marini, K. (eds.)]. MedECC Reports. MedECC Secretariat, Marseille, France, pp. 28, doi: 10.5281/zenodo.10722133, 2024.
- Mendoza, E. T., Jimenez, J. A. and Mateo, J.: A coastal storms intensity scale for the Catalan sea (NW Mediterranean), *Nat. Hazards Earth Syst. Sci.* 11.9, 2453-2462, <https://doi.org/10.5194/nhess-11-2453-2011>, 2011.
- Messner, F. and Meyer, V.: *Flood Damage, Vulnerability and Risk Perception – Challenges for Flood Damage, Flood Risk Management: Hazards, Vulnerability and Mitigation Measures*, 149–167, 2006.
- Moftakhari, H.R., Salvadori, G., AghaKouchak, A., Sanders, B.F., and Matthew, R.A.: Compounding effects of sea level rise and fluvial flooding, *P. Natl. Acad. Sci., USA*, 114, 9785–9790, <https://doi.org/10.1073/pnas.1620325114>, 2017.
- Nagler, T.: *VineCopula: Statistical Inference of Vine Copulas*. R package, available at CRAN, 2012.
- National Academies of Sciences, Engineering, and Medicine (NASEM): *Resilience for Compounding and Cascading Events*, The National Academies Press, Washington, DC., <https://doi.org/10.17226/26659>, 2022.
- Oficina Catalana del Canvi Climàtic (OCCC): *L'impacte de la tempesta Glòria*, 1–6 pp., 2020.



- Palau, R.M., Berenguer, M., Hürlimann, M., and Sempere-Torres, D.: Application of a fuzzy verification framework for the
830 evaluation of a regional-scale landslide early warning system during the January 2020 Gloria storm in Catalonia (NE Spain),
Landslides, 19, 1599–1616, 2022.
- Pérez-Gómez, B., García-León, M., García-Valdecasas, J., Clementi, E., Mösso Aranda, C., Pérez-Rubio, S., Masina, S.,
Coppini, G., Molina-Sánchez, R., Muñoz-Cubillo, A., García Fletcher, A., Sánchez González, J.F., Sánchez-Arcilla, A., and
Álvarez Fanjul, E.: Understanding Sea Level Processes During Western Mediterranean Storm Gloria, *Front. Mar. Sci.*, 8:
835 647437. <https://doi.org/10.3389/fmars.2021.647437>, 2021.
- Petrucci, O. and Llasat, M. C.: Impact of Disasters in Mediterranean Regions: An Overview in the Framework of the HYMEX
Project, *Landslide Science and Practice*, 7, <https://doi.org/10.1007/978-3-642-31313-4>, 2013.
- Pintó, J., Garcia-Lozano, C., Sardá, R., Roig-Munar, F. X., and Martí, C.: Efectes del temporal Glòria sobre el litoral, *Treballs
de la Societat Catalana de Geografia*, 89, 89–109, <https://doi.org/10.2436/20.3002.01.192>, 2020.
- 840 Rivas, V., Garmendia, C., and Rasilla, D.: Analysis of Ocean Parameters as Sources of Coastal Storm Damage: Regional
Empirical Thresholds in Northern Spain, *Climate 2022*, Vol. 10, 10, 6, 88. <https://doi.org/10.3390/CLI10060088>, 2022.
- ROM: Recomendaciones de Obras Marítimas 0.3 Wave Annex E1. Wave climate of the Spanish coast. Puertos del Estado,
1991.
- Romero-Martín, R., Sanuy, M., and Jiménez, J.A.: Unveiling the role of storm surges as a driver of flooding on the western
845 Mediterranean: a case study of the Ebro Delta, *Nat Hazards*, 121, 4961–4984, <https://doi.org/10.1007/s11069-024-06984-5>,
2025.
- Santassusagna Riu, A. and Tort Donada, J.: El temporal Glòria: consideracions sobre la seva afecció a la Costa Central Catalana,
Treballs de la Societat Catalana de Geografia, 89, 191–220, <https://doi.org/10.2436/20.3002.01.196>, 2020.
- Sanuy, M., Rigo, T., Jiménez, J. A., and Llasat, M. C.: Classifying compound coastal storm and heavy rainfall events in the
850 north-western Spanish Mediterranean, *Hydrology and Earth System Sciences*, 25, 6, 3759–3781. [https://doi.org/10.5194/hess-
25-3759-2021](https://doi.org/10.5194/hess-25-3759-2021), 2021.
- Shan, B., Verhoest, N.E.C., and De Baets, B.: Identification of compound drought and heatwave events on a daily scale and
across four seasons, *Hydrol. Earth Syst. Sci.*, 28, 2065–2080, <https://doi.org/10.5194/hess-28-2065-2024>, 2024.
- SMC (Servei Meteorològic de Catalunya): Balanç d'una llevantada històrica a Catalunya, 1–11 pp., 2020.
- 855 Sotillo, M.G., Mourre, B., Mestres, M., Lorente, P., Aznar, R., García-León, M., Liste, M., Santana, A., Espino, M., and
Álvarez, E.: Evaluation of the Operational CMEMS and Coastal Downstream Ocean Forecasting Services During the Storm
Gloria (January 2020), *Front. Mar. Sci.*, 8: 644525, <https://doi.org/10.3389/fmars.2021.644525>, 2021.
- Toomey, T., Amores, A., Marcos, M., and Orfila, A.: Coastal sea levels and wind-waves in the Mediterranean Sea since 1950
from a high-resolution ocean reanalysis, *Front. Mar. Sci.*, 9. <https://doi.org/10.3389/fmars.2022.991504>, 2022.
- 860 Tragsatec and Ministerio para la Transición Ecológica y el Reto Demográfico (MITECO): Guías de adaptación al riesgo de
inundación. Edificaciones, Caso piloto: Ayuntamiento de Los Alcázares (Murcia), 2020.



- Wahl, T., Jain, S., Bender, J., Meyers, S. D., and Luther, M. E.: Increasing risk of compound flooding from storm surge and rainfall for major US cities, *Nature Climate Change*, 5, 1093–1097, <https://doi.org/10.1038/nclimate2736>, 2015.
- Zscheischler, J., Martius, O., Westra, S., Bevacqua, E., Raymond, C., Horton, R. M., van den Hurk, B., AghaKouchak, A., 865 Jézéquel, A., Mahecha, M. D., Maraun, D., Ramos, A. M., Ridder, N. N., Thiery, W., and Vignotto, E.: A typology of compound weather and climate events, *Nat Rev Earth Environ*, 1, 333–347, <https://doi.org/10.1038/s43017-020-0060-z>, 2020.



Appendix A. Complementary tables and maps

870

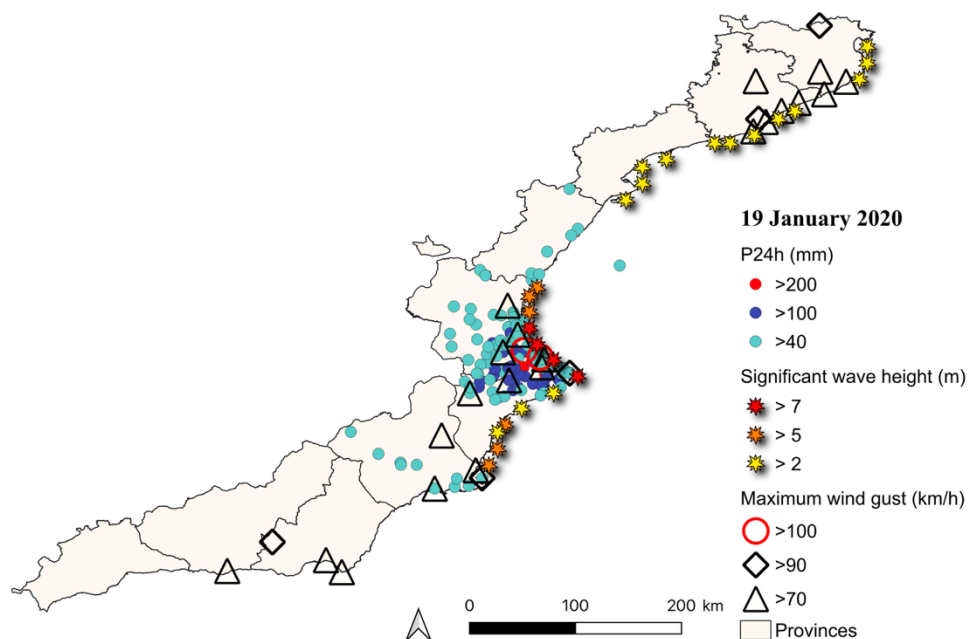
Table A1. Stations that recorded maximum wind gusts above 90 km h⁻¹ between 19 and 21 January *(Coordinates in decimal degrees, WGS84 (EPSG:4326))

Coordinates (Lat, Lon)*	Station name (altitude in m)	Province	19/1	20/1	21/1
38.28° N, 0.57° W	Alicante-Elche aeropuerto (43)	Alicante		94	
41.41° N, 2.12° E	Barcelona - Fabra (408)	Barcelona	91	103	104
41.39° N, 2.2° E	Barcelona - CMT (6)	Barcelona	91	106	
41.29° N, 2.07° E	Barcelona - Aeropuerto (4)	Barcelona		105	
39.01° N, 0.30° W	Barx (340)	Valencia	108	96	
36.72° N, 2.19° W	Cabo de Gata - Faro (52)	Almería		103	
38.78° N, 0.16° E	Jávea -Ayuntamiento (15)	Alicante	93	94	
37.03° N, 2.91° W	Lújar de Andarax (1518)	Almería	93		
40.69° N, 0.16° E	La Pobla de Benifassà (1168)	Castellón			104
42.38° N, 2.75° E	Maçanet de Cabrenys (355)	Girona	94		
41.17° N, 0.35° E	Massaluca (370)	Tarragona		91	
38.95° N, 0.13° W	Miramar - semiautomática (12)	Valencia	100	93	
40.62° N, 0.10° W	Morella - Paseo Alameda (990)	Castellón			97
37.77° N, 0.80° W	Murcia - San Javier II (4)	Murcia		104	
38.92° N, 0.09° W	Oliva (5)	Valencia		115	
41.41° N, 1.51° E	Pontons (632)	Barcelona		91	
37.69° N, 0.73° W	San Javier - La Manga (4)	Murcia	90	91	
39.48° N, 0.47° W	Valencia - Aeropuerto (56)	Valencia		96	
41.50° N, 2.36° E	Vilassar de Dalt (56)	Barcelona	102		



875 **Table A2. Number of municipalities affected by flooding, storm surge, or TCA, by coastal provinces and for the study area as a whole. *In the total figure for each region, each municipality is counted only once, even if it has been affected by one, two or three hazards.**

	GI	BCN	TGN	CAST	VAL	ALIC	MURC	ALM	GRA	MAL	Total
Floods	172	182	68	31	127	66	15	7	3	21	692
Sea storm	18	20	17	13	17	15	2	0	0	0	102
TCA	25	141	28	8	38	10	4	1	0	1	256
Total*	174	218	82	39	142	68	15	8	3	21	770



880

Figure A1. Stations where the wave height, maximum wind gusts and precipitation thresholds were exceeded on 19 January 2020.

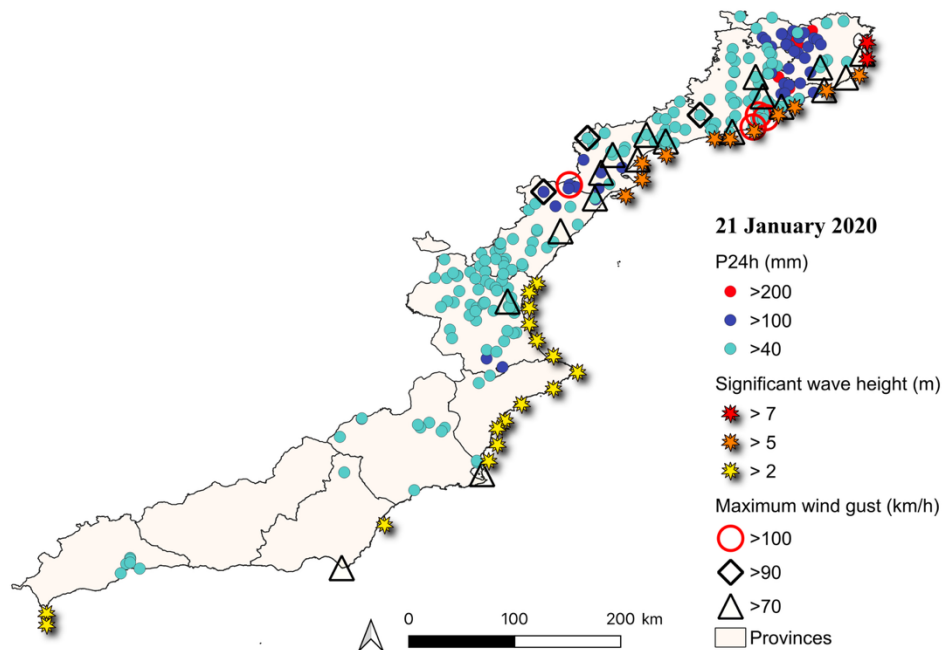
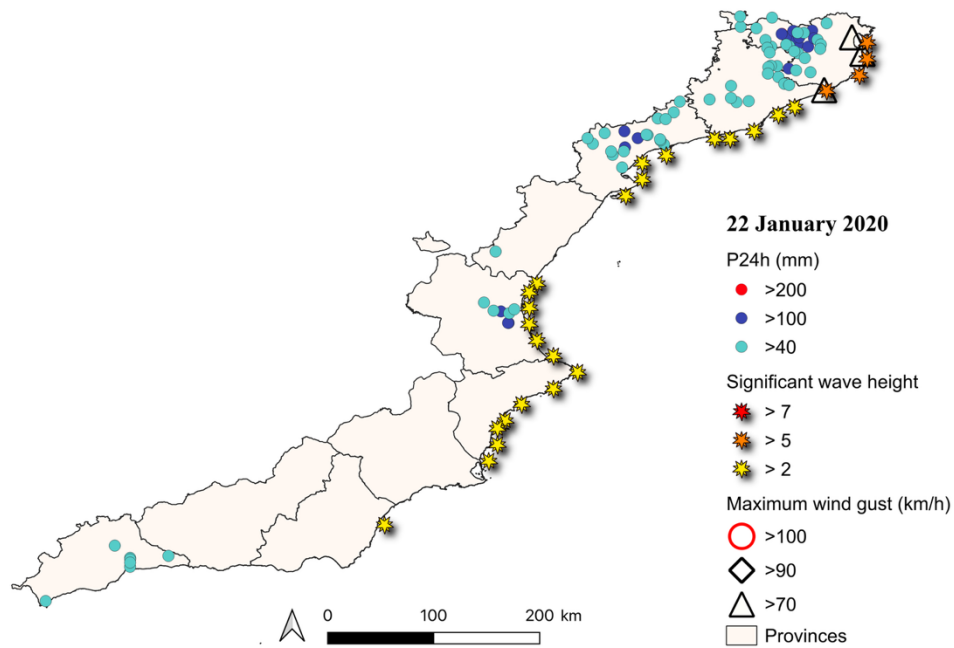


Figure A2. Stations where the wave height, maximum wind gusts and precipitation thresholds were exceeded on 21 January 2020.



885 **Figure A3.** Stations where the wave height, maximum wind gusts and precipitation thresholds were exceeded on 22 January 2020.

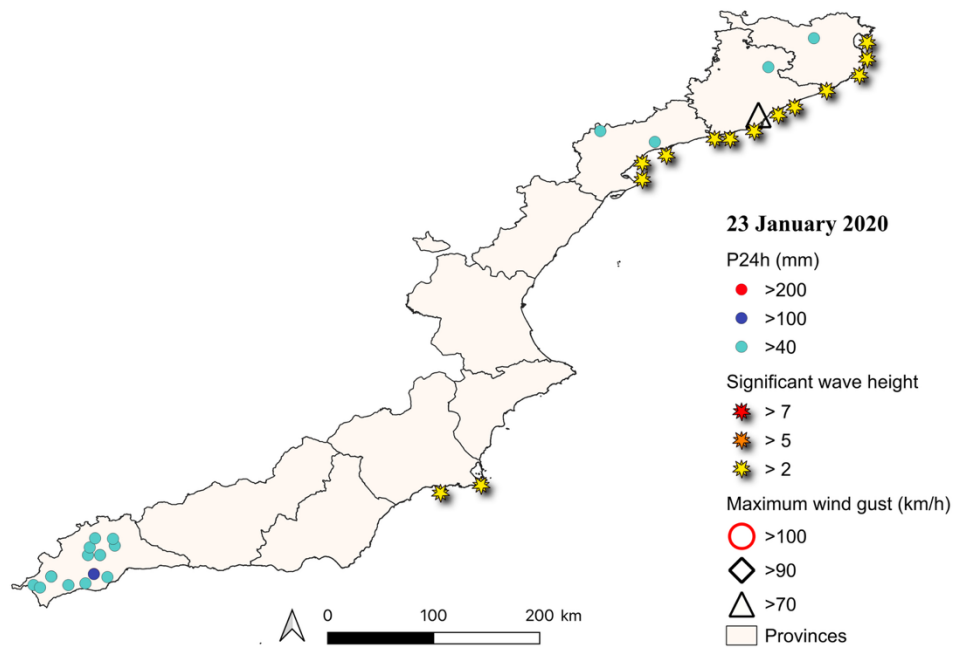


Figure A4. Stations where the wave height, maximum wind gusts and precipitation thresholds were exceeded on 23 January 2020.

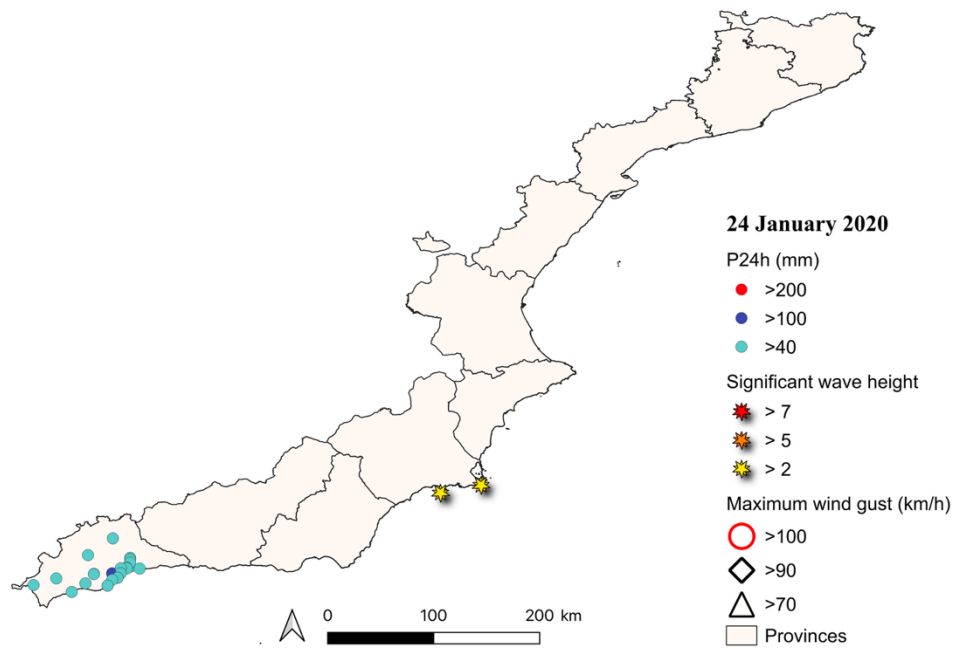
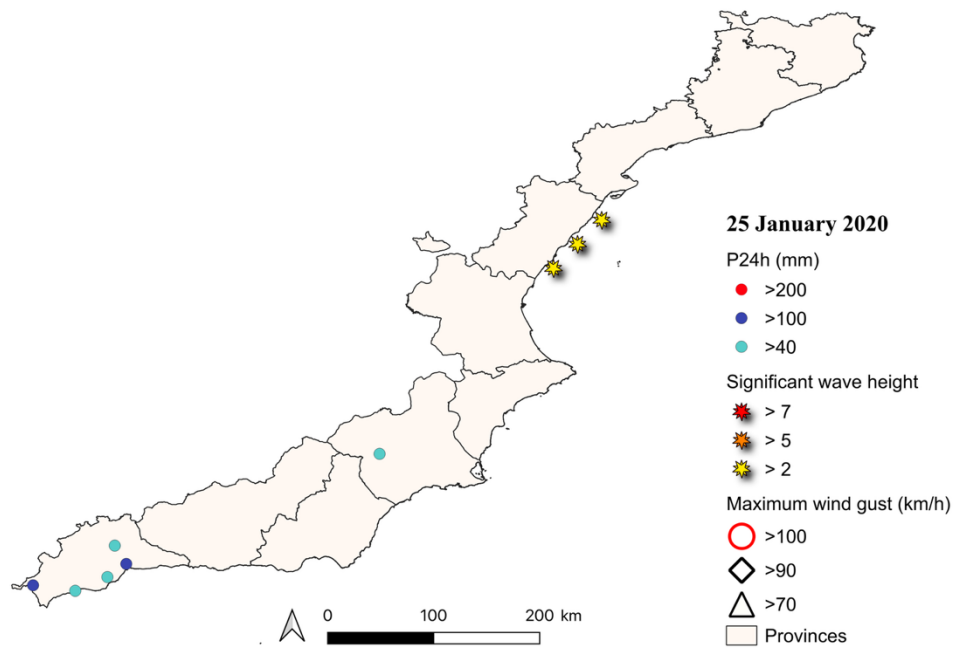


Figure A5. Stations where the wave height, maximum wind gusts and precipitation thresholds were exceeded on 24 January 2020.



890

Figure A6. Stations where the wave height, maximum wind gusts and precipitation thresholds were exceeded on 25 January 2020.